Safety Analysis Calculations for Research and Test Reactors

S. Y. Chen, R. MacDonald and D. MacFarlane
Argonne National Laboratory

XA04C1564

1.0 Introduction

The goal of the RERTR (Reduced Enrichment in Research and Test Reactor) Program[1] at Argonne National Laboratory is to provide technical means for conversion of research and test reactors from HEU (High-Enrichment Uranium) to LEU (Low-Enrichment Uranium) fuels.

In exploring the feasibility of conversion, safety considerations are a prime concern; therefore, safety analyses must be performed for reactors undergoing the conversion. This requires thorough knowledge of the important safety parameters for different types of reactors for both HEU and LEU fuel. Appropriate computer codes are needed to predict transient reactor behavior under postulated accident conditions.

In the following discussion, safety issues for the two general types of reactors, i.e., the plate-type (MTR-type) reactor and the rod-type (TRIGA-type) reactor, resulting from the changes associated with LEU vs. HEU fuels, are explored. The plate-type fuels are typically uranium aluminide (UAl_x) compounds dispersed in aluminum and clad with aluminum. Moderation is provided by the water coolant. Self shut-down reactivity coefficients with HEU fuel are entirely a result of coolant heating, whereas with LEU fuel there is an additional shut down contribution provided by the direct heating of the fuel due to the Doppler coefficient.

In contrast, the rod-type (TRIGA) fuels are mixtures of zirconium hydride, uranium, and erbium. This fuel mixture is formed into rods (~1 cm diameter) and clad with stainless steel or Incoloy. In the TRIGA fuel the self-shutdown reactivity is more complex, depending on heating of the fuel rather than the coolant. The two most important mechanisms in providing this feedback are: 1) spectral hardening due to neutron interaction with the ZrH moderator as it is heated and 2) Doppler broadening of reasonances in erbium and U-238. Since these phenomena result directly from heating of the fuel, and do not depend on heat transfer to the moderator/colant, the coefficients are prompt acting. Results of transient calculations performed with existing computer codes, most suited for each type of reactor, are presented.

2.0 Plate-Type Reactor Fuel

2.1 Safety Limits

The plate-type reactor comprises fuel elements containing fuel plates with thin (less than 1 mm) fuel meat sandwiched between aluminum cladding. Because of the large surface-to-volume ratio of the core, the normal operating temperature of the fuel is generally low (less than 100°C), and the thermal gradient across the plate thickness is very small. Consequently, safety limits for the plate-type reactor rest more on the concerns over: (1) the DNB (departure from nucleate boiling) crisis, and (2) the flow instability crisis. Exceeding either one of these criteria can produce steam blanketing, rapid fuel plate temperature increases, and burnout (plate melting at about 600°C).

The DNB crisis is caused by the continuous formation of steam bubbles on the heated clad surface which eventually blanket the heat-transfer area and inhibit the removal of heat from the fuel. The flow instability phenomenon is reported[2] to be initiated by the detachment of bubbles from the hottest plate in the hot fuel element. Since the detachment and the subsequent formation of bubbles increase the flow resistance through the water channel of the hot fuel plate, some of the hot channel coolant flow is redirected through other cooler channels, resulting in a decrease in flow rate through the hot channel. This tends to enhance the formation of more bubbles and eventually leads to DNB crisis in the hot channel.

Since it appears that flow instability crisis occurs sooner than the onset of DNB during a transient, the former is considered a more stringent limiting criterion in the safety analysis for plate-type reactors, as verified in the calculations discussed in the later section.

2.2 HEU Fuel

Because of the high enrichment, the required uranium loading in HEU fuel is generally low (e.g., 0.6 g/cm^3 for a 10 MW core). The most commonly used fuel material is uranium aluminide (UAl_x-Al).

For the purpose of comparing HEU and LEU cores, the generic 10 MW reactor described in Vol. I of the IAEA Guidebook[3] was selected as a reference design. Several design parameters for this core are shown in Table 1. The HEU core consists of fuel elements with 23 fuel plates each. Design specifications for a standard fuel element are shown in Fig. 1.

For the core using HEU fuel, the calculated fast neutron generation time is 50 μs, and the effective delayed neutron fraction is 0.0077. Various reactivity feedback components are shown in Fig. 2, for both HEU and LEU fuel. As shown, the feedbacks include: the water temperature effect, the water void effect, and the fuel Doppler effect. The water density coefficient, shown in Fig. 2, is equivalent to the water void coefficient for water temperatures below the boiling point. Values for each of the feedback coefficients are shown below.[4]

Effect	$-\delta\rho/\delta T \times 10^{-3}/°C$ (HEU)	$-\delta\rho/\delta T \times 10^{-3}/°C$ (LEU)
Water Temperature (23°C-77°C)	0.121	0.074
Water Density (38°C-50°C)	0.107	0.140
Doppler (20°C-100°C)	0.0	0.026
	0.228	0.240

It is seen that the overall feedback coefficient is lower for HEU. More important, because of the presence of only a small amount of U238 in HEU fuel, the Doppler effect has virtually no contribution to the feedback for HEU.

Several power peaking factors, which would determine the hottest spot in the reactor core, are listed in Table 2 for HEU and LEU fuel. These power peaking factors include: the peak element-to-core average, axial peak-to-average, and peak plate-to-element average. These values were calculated for a flux trap where a 50.0 mm thick water channel was assumed.

2.3 LEU Fuel

For the LEU fuel with 20% enrichment, the required uranium loading is much higher than that for the HEU fuel. For instance, the generic 10 MW LEU core contains a uranium loading varying from 2.27 g/cm^3 to 3.59 g/cm^3. Potential fuel materials to meet this high loading are: UAl_x-Al, U_3O_8-Al, and U_3Si-Al. The high loading of uranium also mandates thicker fuel plates and fewer plates per element, as seen in Table 1.

For LEU fuel using UAl_x-Al, the calculated prompt neutron generation time is 37.7 μs and the effective delayed neutron fraction is 0.0075. The reactivity feedback components are shown in Fig. 2. There is a significant contribution from Doppler effect for LEU that is not available with HEU fuel.

The power peaking factors for LEU are also shown in Table 2, where they are seen to be slightly less than those for HEU.

2.4 Safety Analysis Calculations

This section describes the analytical methods (computer codes), demonstrates their application to the plate-type reactors, and compares the transient behavior of HEU and LEU cores. Since the initiating events for safety analysis are quite system specific, no attempt has been made to define these events in detail. Rather, sample calculations were done for the generic 10 MW reactor for several selected cases within two broad categories: (1) loss of flow transients, and (2) reactivity insertion transients.

2.4.1 Computer Code Selection

Because it is desirable to use a generally available code, the possibility of adapting safety codes commonly used in the nuclear industry for power reactors was investigated. Among the codes considered for plate-type reactors, two of them are found to be most suited in terms of aplicability and availability, i.e., RELAP4/MOD6[5] and COBRA-3C/RERTR.[6] RELAP4 was designed to predict reactor behavior for a variety of accident situations for light-water power reactor systems. In the analysis of power reactors, the code is primarily used to study the system transient response to postulated perturbations such as coolant loop rupture, circulation pump failure, power excursions, etc. RELAP4 models system fluid conditions including flow, pressure, mass inventory, fluid quality, and heat transfer. Component thermal conditions and energy transfers are also modeled. The reactor system is subdivided into discrete volumes which are treated as one dimensional homogeneous elements. RELAP4 solves an integral form of fluid conservation and state equations for each volume and generates a time history of system conditions.

The major attraction of the RELAP4 code for application to research reactors was its coupling of reactor neutronics and thermal-hydraulics models. The neutronics model is point-reactor kinetics. This is coupled with the thermal-hydraulics model through a reactivity feedback model which accounts for the reactivity feedbacks from: Doppler effect of fuel, coolant temperatures effect, and coolant void effect. The fuel element coolant flow and heat transfer from fuel to clad to coolant are predicted from correlations derived for power reactor designs and conditions. The heat-transfer correlations include the Dittus-Boelter correlation for the single-phase, subcooled forced convection regime, and the Thom correlation for the nucleate boiling regime up to a void fraction of 0.80. Since these two heat-transfer correlations are generally applicable and not restricted only to power reactors, the applicability of RELAP4 to the research reactors within the specified ranges is valid.

The COBRA-3C/RERTR code, modified (from COBRA-3C/MIT) at ANL to include plate-type geometry, a flow instability correlation, and a number of DNB correlations applicable to the low pressure regimes typical of research reactor operations, was used to investigate the flow instability and DNB crises under transient conditions. These correlations include the Forgan flow instability correlation and the Macbeth, Labuntsov, Bernath, and Mirshak DNB correlations that are discussed in more detail in Ref. 3. In modeling the plate-type cores with COBRA-3C, a single channel was used to represent the hot channel where the reactor power peaks. The power history was taken from the RELAP4 runs and multiplied by the hot-channel factor to account for the power peaking effect. In the COBRA-3C calculations, the temperatures at the plate centerline and at the clad surface were calculated as functions of time. The plate average temperature as well as the coolant exit temperature were also calculated. The flow instability ratio (FIR) and minimum DNB ratios were calculated as function of time for each transient.

2.4.2 Loss of Flow Transients

Loss of flow transients were calculated starting from full power operation at 10 MW with a coolant flow rate of 1000 m^3/hr, and coolant inlet temperature of 38°C. The coolant flow rate was assumed to decrease exponentially,

$$W = W_o e^{-t/T} ,$$

where,

W = flow rate at time, t,

W_o = flow rate at time t = 0,

T = flow decay parameter.

The flow rate was allowed to decay to a minimum value of 0.25% of full flow and maintained at this level thereafter. Reactor scram was programed to initiate when the flow decreased to 80% of full flow, with a delay time of 0.50 sec for the shut-down reactivity insertion.

HEU Fuel

Results of the loss of flow calculations for T = 1, 5, and 10 sec for HEU fuel have been obtained; however, to avoid lengthy presentation of the details* for each case, only the results for T = 1 sec are presented in Fig. 3 and Fig. 4. The HEU fuel for this case is the 23 plate assembly UAl_x fuel with a uranium loading of 0.6 g/cm^3 and a thermal conductivity of 1.04 W/cm K. As shown in Fig. 3, the flow decrease is initiated at t = 1 sec and has decreased to about 38% of full flow by t = 2 sec. The power decrease starts at about t = 1 sec, initially due to feedback from coolant heating and then drops rapidly at t = 1.7 sec when the control rods move in. As shown in Fig. 4, the maximum fuel temperature increases from the initial steady state value of 85°C to a peak vlue of 102°C, but decreases rapidly to a minimum value of 58°C following reactor scram. As the coolant flow rate continues to decrease, however, the fuel temperature rises again, reaching a value of 90°C at t = 10 sec, when the calculation was terminated. This temperature rise occurs because our model did not provide for shutdown coolant flow by a back up emergency pump or by natural convection. Accordingly, the rise would not occur in an actual reactor which would have provisions for assuring a minimum coolant flow.

---

*Detailed results for T = 5 and 10 sec can be seen in Sec A.6.3.2 on Ref. 4.

Figure 3 also presents the calculated time dependent minimum flow-instability-ratio (FIR) and minimum departure-from-nucleate-boiling-ratios (DNBR) calculated along the hottest fuel plate using the four different correlations available in COBRA-3C/RERTR. They are: the Mirshak correlation, the Labuntsov correlation, the Macbeth correlation at high-velocity regime, and the Bernath correlation. Of these the Mirshak correlation was derived from experiments based on plate-type fuel. As always there is some question about applying correlations derived from steady state experiments to transient conditions, particularly when the rates of change cover a wide range Nevertheless the calculated curves representing the different correlations presented in the figure are interesting because of the wide varitions shown, particularly at normalized flow rates below about 0.20. At initial steady conditions the four correlations give DNB ratios ranging between 7.5 and 15, while the FIR is the most restrictive with a value of 4. Because of the limitations on their applicability we do not recommend that any of the calculated ratios be taken seriously below a normalized flow rate of about 0.05. Indeed because of these limitations, the deviations exhibited at low flow rates are not unexpected. As shown in Fig. 4, the more restrictive ratio at steady state, the FIR, still predicts an adequate margin of safety, with a value of 3, at this low flow rate. All the DNBR correlations, with the exception of Bernath, give DNBR's considerably greater than this.

It was found that for T = 5 and 10 sec transients, the fuel temperature excursions are milder than for the T = 1 sec case, reaching a peak value of 94°C. Also, the slowly decaying flow rates tend to delay the occurrence of both flow instability and DNB crises to much later times.

LEU Fuel

Curves for the loss of flow calculations for LEU fuel are again shown for T = 1 sec case (Fig. 5 and Fig. 6). The LEU fuel for this case is the 19 plate assembly UAl_x fuel with a uranium loading of 2.27 g/cm^3 and a thermal conductivity of 0.69 w/cm K. As can be seen by comparing these figures with the earlier curves (Figs. 3 and 4) for HEU fuel, the results are virtually the same for LEU fuel, as would be expected. The difference that does exist is due to slightly greater negative reactivity feed-back, prior to scramming the reactor, for the LEU fuel. This shows up as a slightly greater initial power decrease prior to reactor scram. As a result of this, the peak fuel temperatures achieved with the LEU core are a few degrees lower for the same transient. These small differences can be seen by comparing the reactor power and fuel temperature curves between LEU and HEU cases for the various transients.

The conclusion to be drawn from this series of loss of flow calculations is that it would be difficult to exceed a peak fuel temperature much above 100°C even for a sudden flow stoppage, as long as the reactor is scrammed. When the flow decay occurs on a time scale of tens of seconds, as would be more characteristic of a realistic pump coastdown, the peak fuel temperatures are even less. There is a negligible difference between HEU and LEU fueled cores.

2.4.3 Reactivity Insertion Transients

Reactivity insertion calculations started from an initial condition with the reactor just critical at 1 watt and at a uniform temperature of 38°C with full coolant flow. The reactor response to step inputs of $1.1 and $1.2 without reactor scram was calculated for the following HEU and LEU fuels:

1. HEU - 23 plate assembly with 0.6 g/cm^3 U loading in UAl_x fuel; k = 1.04 w/cm K
2. LEU - 19 plate assembly with 2.27 g/cm^3 U loading in UAl_x fuel; k = 0.69 w/cm K
3. LEU - 19 plate assembly with 2.27 g/cm^3 U loading in U_3O_8 fuel; k = 0.48 w/cm K
4. LEU - 19 plate assembly with 3.0 g/cm^3 U loading in U_3O_8 fuel; k = 0.14 w/cm K.

In each case the core was assumed to be completely loaded with the given fuel, and the power peaking factors and reactivity feedback coefficients associated with the fuel (Fig. 2) were used.

HEU Fuel

Curves showing the calculated response of the HEU fueled 10 MW reactor to a step input of $1.1 are presented in Figs. 7 to 9. As shown in Fig. 7, the initial reactor power peak of 40 MW is turned around by negative reactivity feedback at about 0.9 sec after the step insertion. Thereafter the power rises steadily because of the absence of a reactor scram, eventually exceeding the initial peak at t = 4 sec. The power rise after the initial peak would not occur in an actual reactor since a reactor scram would have occurred and terminated the power rise.

The calculated peak fuel temperature (Fig. 8) shows an initial maximum of 132°C at t =1 sec, followed by a drop of about 12°C, and then a steady rise because of the increase in reactor power above the 10 MW level. In an actual reactor transient the second rise would not occur because the reactor would be scrammed by the safety system.

Figure 9 presents the minimum DNBR and FIR calculated along the hottest fuel plate during the transient. As in the flow transients, the FIR is more restrictive than the DNBR given by the Mirshak correlation, although the difference between the two is much smaller at the full flow conditions maintained throughout this power transient. As shown, the FIR drops below 1.0 at t = 4 sec, when the reactor power is 4 times design, or 40 MW. This is also the time when the coolant exit temperature exceeds 100°C (Fig. 8). Bulk coolant boiling begins at t = 6.6 sec when the saturation temperature for the reactor exit pressure of 20 psig is exceeded.

Similar results for a step reactivity insertion of $1.2 were also calculated. The major difference for this case is a more rapid initial power rise (to 140 MW in 0.56 sec) and a higher peak fuel temperature (222°C). In contrast to the $1.1 step case, the initial power peak produces an initial reduction in the FIR that drives it below 1.0. Thereafter the FIR recovers briefly above 1.0, and drops below 1.0 at t = 2 sec when the reactor power is 40 MW and the coolant exit temperature has just exceeded 100°C. This latter behavior is consistent with the results for the $1.1 transient.

LEU Fuel

The same set of calculations described above were run for the LEU core comprised of the 19 plate aluminide fueled assemblies. Aside from the differences in fuel plate spacing and thickness, as compared to the HEU core, the major difference is the prompt component of reactivity feedback due to the Doppler effect in the 20% enriched fuel (Fig. 2). Additionally, the LEU fuel core has a somewhat shorter prompt neutron lifetime, which leads to a more rapid response in super prompt critical transients.

Figure 10 presents the calculated response of reactor power to the \$1.1 step insertion. As shown, the power increases to an initial peak of only 28 MW, 0.73 sec after the reactivity insertion. The corresponding initial peak fuel temperature is about 103°C at t = 1 sec (Fig. 11). This compares with a peak power of 40 MW at 0.9 sec and a peak fuel temperature of 130°C with the HEU fuel for the same transient.

Calculated DNBR and FIR ratios (Fig. 12) show trends similiar to those for the other transients, namely a decrease in the FIR to 1 when the power reaches 4 times normal, or 40 MW and the coolant exit temperature exceeds 100°C. Because the power rise is slower, the coolant has not reached bulk boiling by the time the calculation was stopped at t = 10 sec.

Similar calculations for a \$1.2 step insertion have shown that power initially increases to 90 MW in 0.44 sec before being turned around by the combined prompt Doppler and delayed coolant density feedback coefficients. The initial peak fuel temperature was 130°C. These values compare with a peak power of 140 MW in 0.56 sec and a peak fuel temperature of 222°C for the same transient with HEU fuel.

The calculated FIR and DNBR show results consistent with the earlier transients namely, the FIR drops to 1.0 when the reactor power reaches 40 MW and the coolant outlet temperature exceeds 100°C. As in the \$1.1 transient with LEU fuel, the coolant has not reached the boiling temperature at the time the calculation was stopped.

To investigate the effects of varying fuel properties on the LEU fueled reactor transient response, two additional cases were run with a \$1.2 step reactivity input. The results for the first case, which is based on U_3O_8-Al dispersion fuel with a uranium loading of 2.27 g/cm^3, were calculated. For this case the fuel thermal conductivity was reduced to 0.48 W/cm K, an appropriate value for U_3O_8 dispersion fuel (see Section A.2 of Ref. 4). All reactor kinetics, reactivity feedback and power distribtion parameters are the same as those used for the other cases with LEU fuel. The initial reactor power peak of 95 MW was reached in about 0.44 sec before being turned around by the negative feedback. The reactor power trace is virtually identical to that for the LEU higher thermal conductivity aluminide fuel for a \$1.2 insertion. The corresponding peak reactor fuel temperature was 130°C, which is only a few degrees higher than the temperature for the aluminide fuel. The calculated FIR and DNBR ratios showed the same result as in the other transients. The FIR decreases to 1.0 when the reactor power reaches 40 MW and the coolant exit temperature exceeds 100°C at t = 6 sec.

The second of the two additional cases was run for a U_3O_8 dispersion-type fuel with a thermal conductivity (0.14 W/cm K) correspondng to a uranium loading of 3.0 g/cm^3 in order to investigate the sensitivity of transient parameters to a further decrease in thermal conductivity. All other reactor parameters, including the power peaking factors, remained the same as for the case with a uranium density of 2.27 g/cm^3. It was shown by the calculation that the reactor power trace is relatively unaffected by this change, again reaching 94 MW in about 0.4 sec. The peak fuel temperature, however, is increased about 17°C to 147°C. Also, the difference between the clad and peak fuel temperature is greater as the power increases after the initial spike.

The trend with the FIR and DNBR, is as in all the earlier transients, with the FIR reaching a value of 1.0 when the reactor power is at 40 MW. As compared with the other $1.2 LEU cases, the power rise after the initial peak is slower, reaching 40 MW in 7 sec instead of 6 sec.

3.0 Rod-Type Reactor Fuel

3.1 Safety Limits

Unlike the plate-type reactor, the rod-type (TRIGA) reactor comprises fuel bundles containing uranium-zirconium hydride fuel rods with a relatively large diameter (>1 cm). The thickness of the fuel pin, combined with the existence of a gap between fuel and cladding, tends to develop a relatively high operating temperature (>300°C for a 14 MW TRIGA) and a large thermal gradient across the pin radius. This high temperature level is further enhanced in the hot fuel pin where several power-peaking factors are superimposed.

In addition to the usual power peaking caused by nonuniform radial and axial power distributions, a highly skewed power peaking caused by local flux peaking is found to exist in the fuel pin adjacent to a large in-core water cavity(for experiment access). Consequently, in contrast to the DNB* crisis discussed above for plate-type fuel, temperature of the hottest fuel pin sets the limiting conditions for a rod-type reactor. This is because the rod-type fuel, having a thicker cross section and lower thermal conductivity, has a much lower time constant for heat transfer. Therefore, in a power transient, a limiting peak fuel temperature is usually reached before the heat flux at the rod surface increases enough to produce the DNB crisis. With the TRIGA fuel, this peak temperature limit is determined by the dissociation pressure of the zirconium hydride and is about 750°C.

3.2 HEU Fuel

Since the rod-type reactors under consideration here are TRIGA's manufactured by the General Atomic Company, a 14 MW TRIGA was selected for comparison between HEU and LEU cores. This allows a close comparison of the results derived from this study and those from the existing TRIGA reactors[7] currently in operation. Design specifications for a fuel element (5 x 5 array) are given in Fig. 13.

The fuel material for TRIGA reactors is uranium-erbium-zirconium hydride alloy. The presence of erbium contributes largely to the negative reactivity (Doppler) feedback. This feedback coefficient is shown in Fig. 14, where it is displayed over the fuel temperature range from 0°C to 900°C. Unlike the plate-type fuel, feedback components from coolant are insignificantly small for the TRIGA reactors.

*Since the coolant is allowed to mix freely between subchannels for the rod-type reactor, the flow instability crisis does not apply to a TRIGA-type reactor.

The power peaking factors that determine the hottest spot in the core are,

Core axial peak/average	1.35
Core radial peak/average	1.9 (or 2.5)
Hot-pin radial peak/average =	2.12
Total	5.44 (or 7.16)

The last power peaking factor is determined by the skewed power profile in the hottest pin mentioned in the previous section. This power profile is shown in Fig. 15 along the radial axis and in Fig. 16 over the azimuthal angle. It is seen that the power peaks near the pin edge facing the water cavity.

Two important neutronic parameters calculated for the HEU core at end of life (EOL) are the fast neutron generation time (39 μs) and the effective delayed neutron fraction (0.007).

3.3 LEU Fuel

A study of the generic TRIGA reactors [3] has revealed that the original HEU core configuration can remain unchanged while the uranium loading is raised to meet the loading requirement for the LEU core. Thus, the relevant changes in relation to the safety concerns involve only the neutronic and thermal properties of the fuel.

For LEU, the feedback coefficient is shown in Fig. 13. The curve for HEU is also shown for comparison. The trend shows a stronger feedback contribution from HEU for fuel temperature greater than about 300°C. The skewed power profile is also affected. As shown in Fig. 15, the power peaks at 2.52 for the LEU fuel. The neutron lifetime was found to be 32 μs at EOL, and the effective delayed neutron lifetime remains the same (i.e., 0.007).

Thermal properties specifically for the LEU fuel were not available, so it was assumed that the changes from HEU are not great, and the effect on results is not significant.

3.4 Safety Analysis Calculations

3.4.1 Computer Code Selection

For the purpose of calculating the power trace and DNB ratios, both RELAP4 and COBRA-3C codes, descibed in Section 2.4, were also applied to the TRIGA reactor calculations. Procedures used for modeling the TRIGA reactor by these two codes were similar to those described for the plate-type reactor, except that the TRIGA parameters and appropriate configuration were used. In addition to RELAP4 and COBRA-3C, a conduction code (HEATING5) was employed.

HEATING5[7] is a multi-dimensional, time-dependent code, designed to perform detailed heat conduction calculations for non-uniform source distributions in heterogeneous media. In applying the code, the boundary conditions between the medium interfaces are to be supplied. Also, the power history is also supplied externally (from the RELAP4 run). HEATING5 is needed to carry out the detailed temperature distribution calculations in the hottest fuel pin where the skewed power profile due to flux peaking produces a highly asymmetric heat source. Provision for this asymmetric source input is not available in either RELAP4 or COBRA-3C. The model of the hottest pin used in the HEATING5 calculations is shown in Fig. 17, where the mesh intervals are taken on the cross section at the axial midplane of the rod. In the calculation, the power density corresponding to the skewed profile (see Figs. 15 and 16) was input as the heat source for each node.

3.4.2 Loss of Flow Transients

In this accident, it is postulated that the coolant flow rate through the core is coasting down from the full rate of 8,000 gpm to the 300 gpm rate maintained by the emergency pump. The flow rate as a function of time is assumed to follow an exponential form characterized by the coastdown time, T. That is, at time t seconds after the accident, the flow rate W is described by,

$$W(t) = 8000 \exp(\lambda t) \quad \text{gpm, for } t < T,$$
$$= 300 \quad \text{gpm, for } t > T,$$

where $\lambda = \frac{\ln (300/8000)}{T}$.

The following conditions were assumed in this calculation: (1) the reactor is at full power of 14 MW; (2) the core-radial peaking factor is 2.1; (3) the reactor scrams on low-flow (less than 7,000 gpm) signal; (4) control rod motion is delayed for 0.2 seconds following a scram signal.

<u>HEU</u>

Calculations were carried out for coastdown times ranging from 1 to 15 seconds. The power trace of the average core following scram was first calculated by RELAP4, and is shown in Fig. 18 for the hot pin with radial peak/average factor of 2.5. This power trace was fed into COBRA3C/RERTR for cases corresponding to different values of the coastdown time, T. In these calculations, the Mirshak correlation was used to determine the DNB ratio results which are presented in Table 3 for core-radial peaking factors of 1.9, 2.1, and 2.5.

The COBRA results in Table 3 indicate that DNB is reached for T equal or less than 3 sec for the peaking factor of 1.9. For higher power-peaking factors, DNB occurs at higher flow coastdown times. A check of the results can be seen from Fig. 19, where the similar coastdown situations were followed by a different approach,[7] using a core-radial peaking factor of 2.0. In Fig. 19, a somewhat optimistic result, i.e., no DNB for T = 2 sec, was predicted.

<u>LEU</u>

No major differences were found for LEU in the flow transient cases. The results presented in Table 3 for HEU remain essentially unchanged for LEU.

3.4.3 Reactivity Insertion Transients

Reactivity insertion calculations included two separate cases: (1) Step insertion from 1W with the reactor critical and a very low flow rate, (2) Step insertion from full power with full flow rate. The reactor responses to a step input of 1% $\delta k/k$ in case (1) and 1% $\delta k/k$ and 0.75% $\delta k/k$ in case (2) were obtained. In the calculations, scram was assumed to function. The power setpoints of 3.6 MW and 14.7 MW were chosen for case (1) and (2), respectively. A 0.2 sec delay between scram signal and start of rod motion was assumed. Temperature-dependent thermal properties were used, with specific heat of the fuel given by $Cp = 0.086 + 10^{-4}$ T cal/gm-C and fuel conductivity by $k = 0.042 + 1.79 \times 10^{-5}$ T cal/sec C, where T is the fuel temperature in °C.

HEU

For the transient described by case (1), the power trace calculated by RELAP4 is presented in Fig. 20, where a peak of 448 MW is found to occur at t = 0.52 sec. Similar calculations without scram action are also shown in the same figure. It is seen that in both cases the power rise is turned by the negative temperature feedback. During the transient, the maximum average core temperature was 232°C. The power history from RELAP4 was input to HEATING5 to calculate the fuel temperature distribution in the hottest pin. It was found that a peak temperature of 691°C was reached at node 7 when the power peaks (see Fig. 21).

For the case (2) transient, a peak power of 281 MW occurs at 0.3 sec after the insertion of reactivity. With the reduction in shim-bundle worth from 1% $\delta k/k$ to 0.75% $\delta k/k$ the peak power drops to 119 MW (see Fig 22). The peak power achieved in this accident is considerably lower than in the similar accident discussed above. This is because feedback coefficients are higher at high fuel temperatures and thus serve to suppress the rise of power to a greater extent. In the RELAP4 calculations, the maximum average core temperatures were 389°C and 342°C for the shim-bundle worths of 1% $\delta k/k$ and 0.75% $\delta k/k$, respectively.

The HEATING5 calculations for this transient used the convective heat transfer coefficients corresponding to the full-flow case. The calculated time history of fuel temeratures are presented in Fig. 23 for the step worth of 1% $\delta k/k$. A peak temperature of 909°C was located at node 6 (described in Fig. 17). For the step worth of 0.75%, a peak of 792°C was found at node 4, which is farther from the edge of the pin than in the same transient from low power. This is primarily attributable to the large temperature gradient already established at the edge prior to the transient, causing the peaking location to shift away from the edge during the transient. A large temperature drop across the clad is also observed in this transient case.

LEU

Figure 24 presents power versus time histories for transient case (1), calculated by RELAP4 for both scram and no-scram situations. Peak power in both cases reached 460 MW at 0.52 sec. The maximum average core temperature calculated was 210°C.

Figure 25 shows the HEATING5 results on node 7 (where peak temperature occurs), the centerline temperature, and the pin-average temperature. The peak temperature calculated was 671°C.

Figure 26 presents the power versus time histories for case (2) transients with step worths of 1% $\delta k/k$ and 0.75% $\delta k/k$. Peak power reached in the former is 427 MW and the latter, 119 MW. The respective maximum core-average temperatures calculated by RELAP4 were 426°C and 353°C.

The HEATING5 results for fuel temperatures are presented in Fig. 27 for the same case with shim-bundle worths of 1% $\delta k/k$. Similar to the situation for the HEU fuel, the peak temperatures in both cases were located at node 6 and node 4 for shim-bundle worths of 1% $\delta k/k$ and 0.75% $\delta k/k$, respectively. They are 1050°C and 841°C for the shim-bundle worths of 1% $\delta k/k$ and 0.75% $\delta k/k$, respectively.

4.0 Conclusions

With proper selection of existing computer codes and the ranges of applicability, methods previously used for power reactor transient calculations can be adapted to applications for research and test reactors with satisfactory results. Further verification will be conducted by comparison against experimental test results, such as the SPERT tests.

From the results shown in the loss of flow transients with reactor scram, it can be concluded that for sudden stoppage of flow in a matter of one or two seconds, the safety limit may be violated for both the plate-type and rod-type reactors. However, a longer coastdown period (say, greater than 10 sec) would prove to be benign.

For plate-type reactors the conclusions to be drawn from the series of reactivity insertion transients are that the LEU fueled cores show a more rapid power turn around, with a lower peak power and lower fuel temperatures, because of the significant prompt Doppler feedback due to fuel heating. This lower peak power, combined with the lower power density due to the thicker fuel meat, results in lower peak temperatures in the LEU fuel. To verify the accuracy of the calculations the models used must be validated or benchmarked. In spite of this, the comparative behavior of the two types of cores should be qualitatively correct.

As shown by the calculations, the response of the LEU fuel core is insensitive to reduced fuel conductivity. In the calculation of response to a \$1.2 input, a reduction of the conductivity of the U_3O_8 fuel by a factor of 3.5 gave a slight decrease in the peak of the power pulse, from 94 to 93 MW, and an increase in peak fuel temperature from 130 to 147°C. Although a stronger Doppler feedback is anticipated by the increase of fuel temperature due to the lowering of conductivity, the magnitude is somewhat offset by a weaker feedback from coolant due to the poorer heat transfer.

Although peak temperatures in TRIGA reactors during reactivity transients have been shown to be higher for LEU than for HEU, these differences are acceptable.

Our overall conclusion, based on these results, is that there appear to be no particular safety problems associated with the LEU fueled cores. The differences that do exist are for the most part in the direction of improved safety with the LEU fuel.

References

1. Travelli, A., "Current Status of the U.S. RERTR Program," Trans. Am. Nucl. Soc., Vol. 33, pp. 737-738 (1979).

2. Essler, W. A. and Kreyger, P. J., "Flow Instability in HFR Fuel Element Cooling Channels," RCN-Int-69-018, Reactor Centrum Netherland, Petten (March 1969).

3. IAEA Guidebook on Research and Test Reactor Conversions From the Use of HEU to the Use of LEU Fuels, Vol. I, Draft 4, International Atomic Energy Agency (December 1979).

4. IAEA Guidbook on the Safety and Licensing Aspects of Research Reactor Core Conversion from HEU to LEU Fuels, Appendix A, Draft 1 (September 1980).

5. RELAP4/MOD6, A Computer Program for Transient Thermal-Hydraulic Analysis of Nuclear Reactors and Related Systems User's Manual, EG&G Idaho, Inc. (January 1978).

6. Chao, J., et al., "COBRA-3C/RERTR: A Thermal-Hydraulic Subchannel Code with Low Pressure Capabilities," Science Applications, Inc. (Sept. 1979).

7. Safety Analysis Report of the TRIGA Steady-State Research/Materials and Test Reactor for the Institute for Nuclear Technologies, Bucharest, Romania, E-117-232, Vol. II, General Atomic Company, (February 1974).

8. Turner, W.D., "HEATING5 - AN IBM 360 Heat Conduction Program," ORNL/CSD/TM-15, Oak Ridge National Laboratory, Oak Ridge, Tennessee (1977).

Table 1

10 MW Reactor - Cycle Length Matching Criterion (16.7 Days)
Fuel Element Design Variations With 20% Enriched Uranium Fuel[a]

Number of Plates	Enrichment, %	$H/^{235}U$, Std. Element[b]	Thickness of meat, mm	Thickness of Water Channel, mm	Volume of Meat cm^3/Element	Uranium Density, g/cm^3	^{235}U Density, g/cm^3	wt.% U[c]	^{235}U per Element, grams
23	93	196	0.51	2.188	443	0.68	0.632	22	280
23	20	172	0.51	2.188	443	3.59	0.718	66.3	318
21	20	145	0.839	2.188	666	2.60	0.523	56.6	346
19	20	207	0.51	2.916	366	3.96	0.792	69.2	290
19	20	184	0.70	2.726	503	3.05	0.610	61.4	307
19	20	171	0.80	2.626	575	2.77	0.554	58.6	319
19	20	158	0.90	2.526	646	2.56	0.512	56.2	331
19	20	145	1.00	2.426	718	2.42	0.483	54.4	347
19[a]	20	113	1.238	2.188	889	2.27	0.453	52.6	403
18	20	97	1.471	2.188	1001	2.23	0.445	52.1	446
17	20	83	1.731	2.188	1112	2.24	0.448	52.2	498

[a]All calculations in the table were done with microscopic cross sections corresponding to the fuel element with average burnup in the core. To investigate changes in cycle length and uranium density in the fresh feed elements due to cross section variation with burnup, the calculations for both the reference 93% enriched case and the 19 plate case with 1.238 mm thick fuel meat were repeated for extreme values of the cross sections. With microscopic cross sections corresponding to slightly-burned (i.e., at equilibrium Xe and Sm) fresh elements, the cycle length in both the 93% and the 20% enriched cases was 15.9 days, and the uranium density in the fresh feed elements of the 20% enriched case was 2.26 g/cm^3. With microscopic cross sections corresponding to elements with the discharge burnup, the cycle length in both the 93% and 20% enriched cases was 17.4 days, and the uranium density in the fresh feed elements of the 20% enriched case was 2.24 g/cm^3.

[b]Includes a 1 mm water channel surrounding each element.

[c]Porosity of 10 volume percent assumed with 20% enriched UAl_x-Al fuel.

Table 2. Power Peaking Factors

	HEU Flux Trap 50.0 mm	LEU Flux Trap 50.0 mm
Radial	1.63	1.38
Axial	1.31	1.31
Local	1.23	1.34
Total	2.63	2.41

Table 3. Results of COBRA-3C/RERTR Calculations for Coastdown Accidents

Coastdown Time (sec)	Core Radial Power Peaking Factor	Minimum DNB Ratio	Time to Exceed CHF (sec)	CHF* (10^6 Btu/hr-ft^2)
1.0	1.9	----	0.9	0.19
2.0	1.9	----	1.8	0.17
3.0	1.9	----	3.6	0.11
4.0	1.9	1.26	---	0.12
5.0	1.9	1.65	---	0.13
15.0	1.9	2.74	---	1.57
4.0	2.1	1.02	---	0.10
5.0	2.1	1.35	---	0.12
15.0	2.1	2.39	---	1.60
4.0	2.5	----	3.2	0.20
5.0	2.5	----	5.6	0.11
15.0	2.5	1.95	---	1.56

*Critical Heat Flux at time of minimum DNBR or time CHF exceeded.

FIGURE 1. 10 MW Reactor - Standard[a] (23 Plates/Element) and Control[a,b] (17 Plates/Element) Fuel Elements.

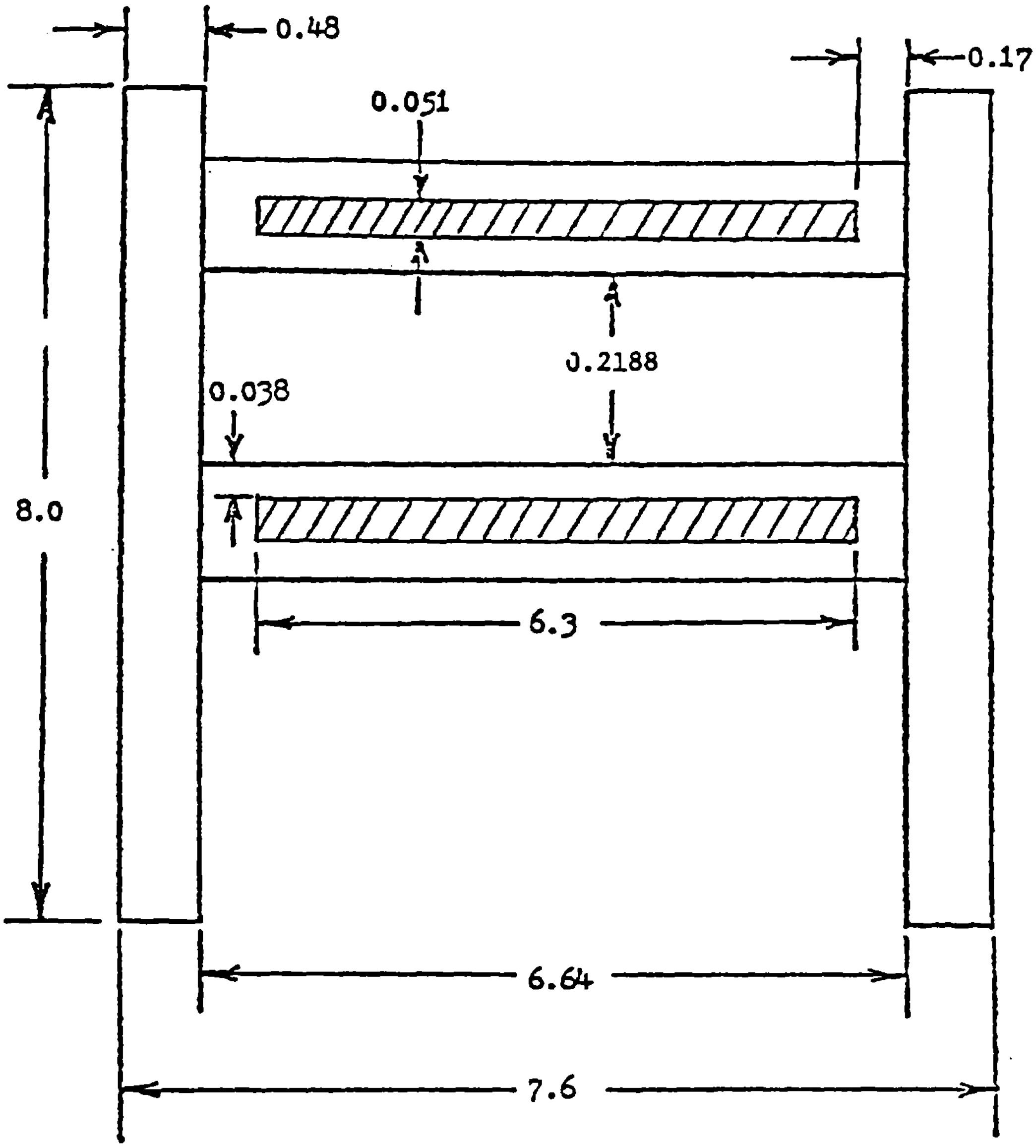

All dimensions in cm.

[a]The two outermost plates have a clad thickness of 0.0495 cm.
[b]Control fuel elements have four Al plates/element, assuming two fork-type absorber blades/element.
[c]Including a 1 mm water channel surrounding each element.

VOLUME FRACTIONS[c]

Standard Fuel Element		Control Fuel Element	
Fuel Meat	0.1185	Fuel Meat	0.0876
Aluminum	0.3205	Aluminum	0.3244
Water	0.5610	Water	0.5880

Figure 2. Isothermal Reactivity Feedback Data Corresponding to changes in Water Temperature only, Water Density Only, Doppler effect only and Water Voidage Only for HEU and LEU Cores

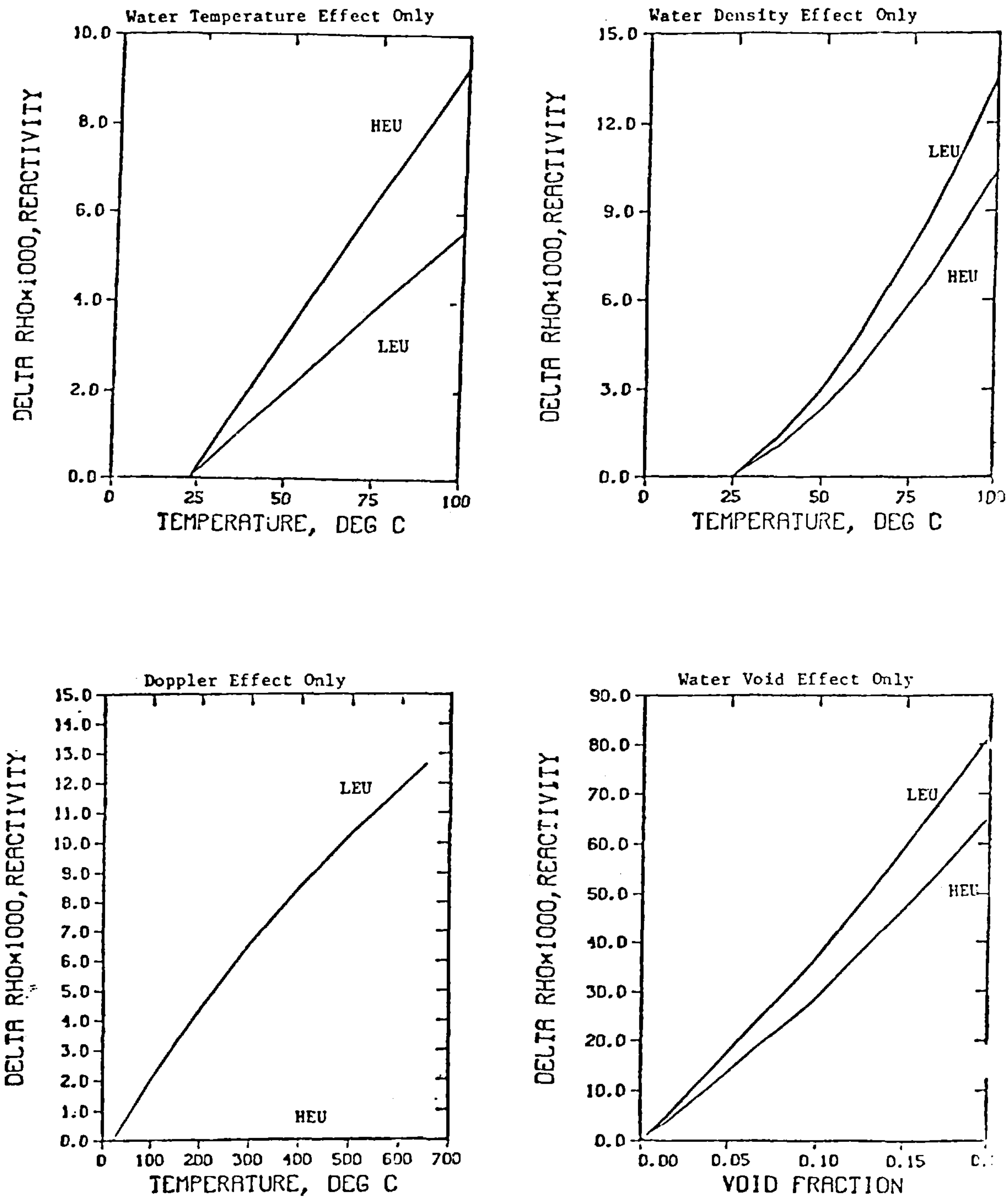

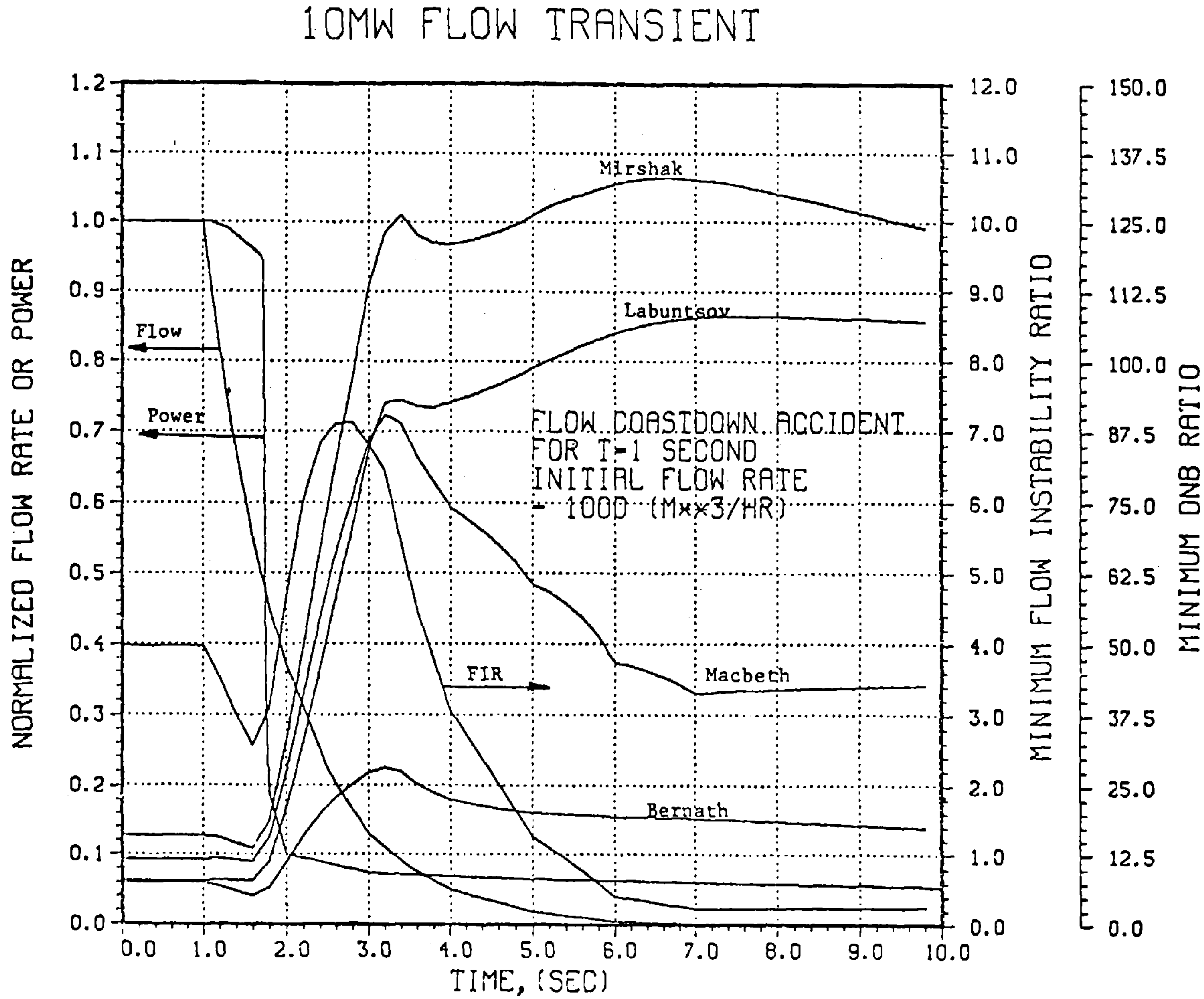

Figure 3. Loss of Flow Transient, HEU Fuel, T = 1 sec
Time Histories of Power, Flow, FIR, and DNBR

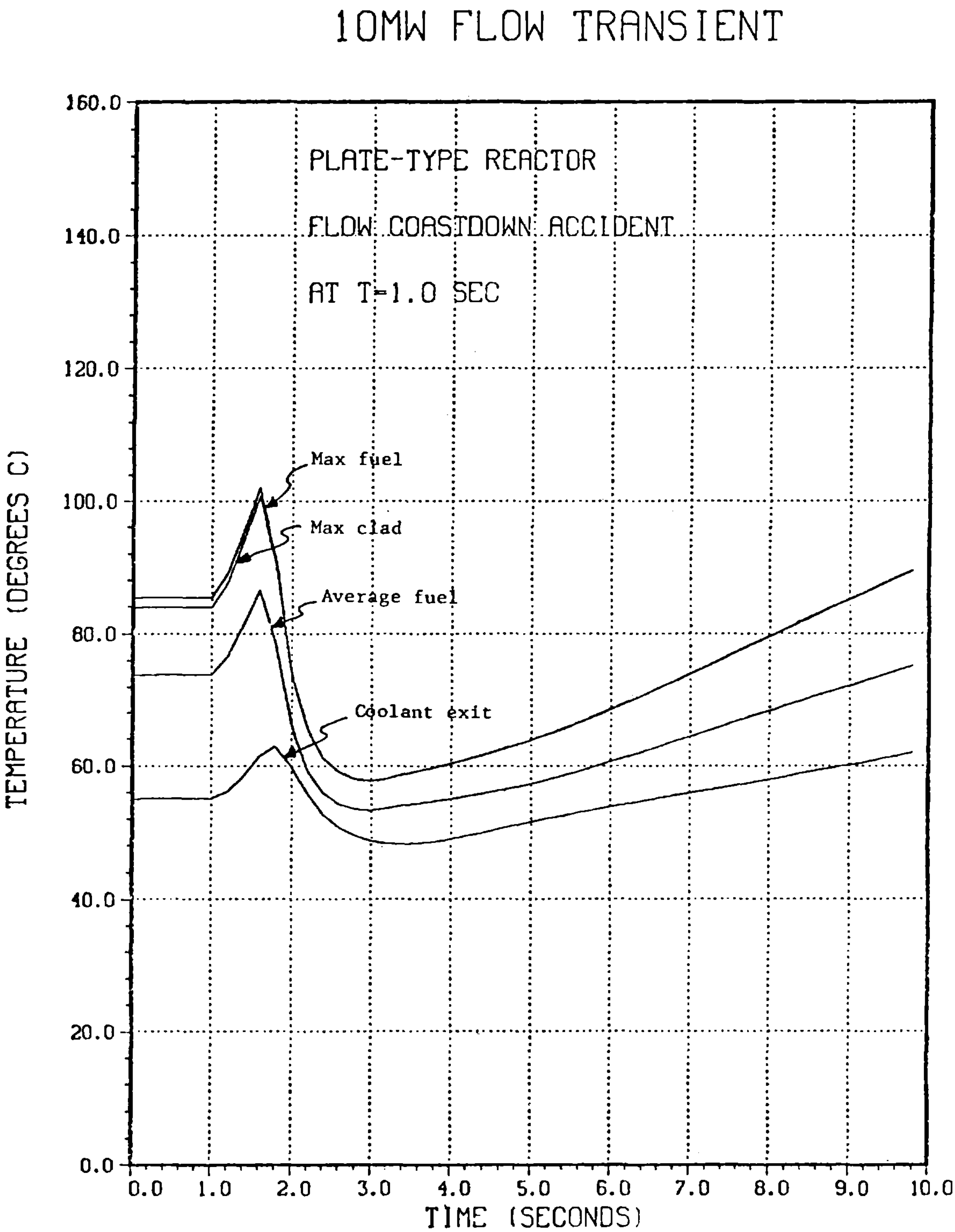

Figure 4. Loss of Flow Transient, HEU Fuel, T = 1 sec
Time Histories of Fuel and Clad Temperatures

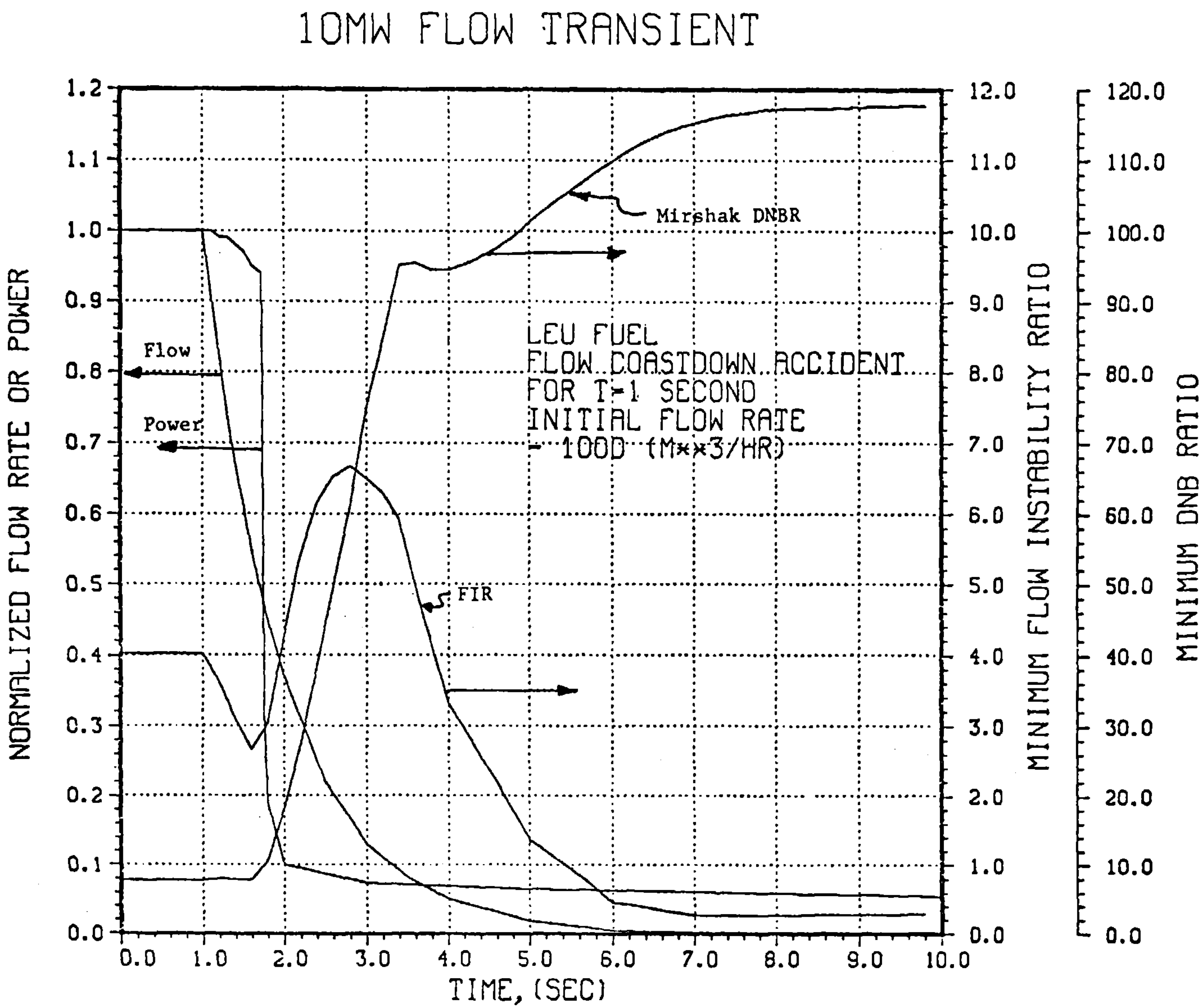

Figure 5. Loss of Flow Transient, LEU Fuel, T = 1 sec
Time Histories of Power, Flow, FIR, and DNBR

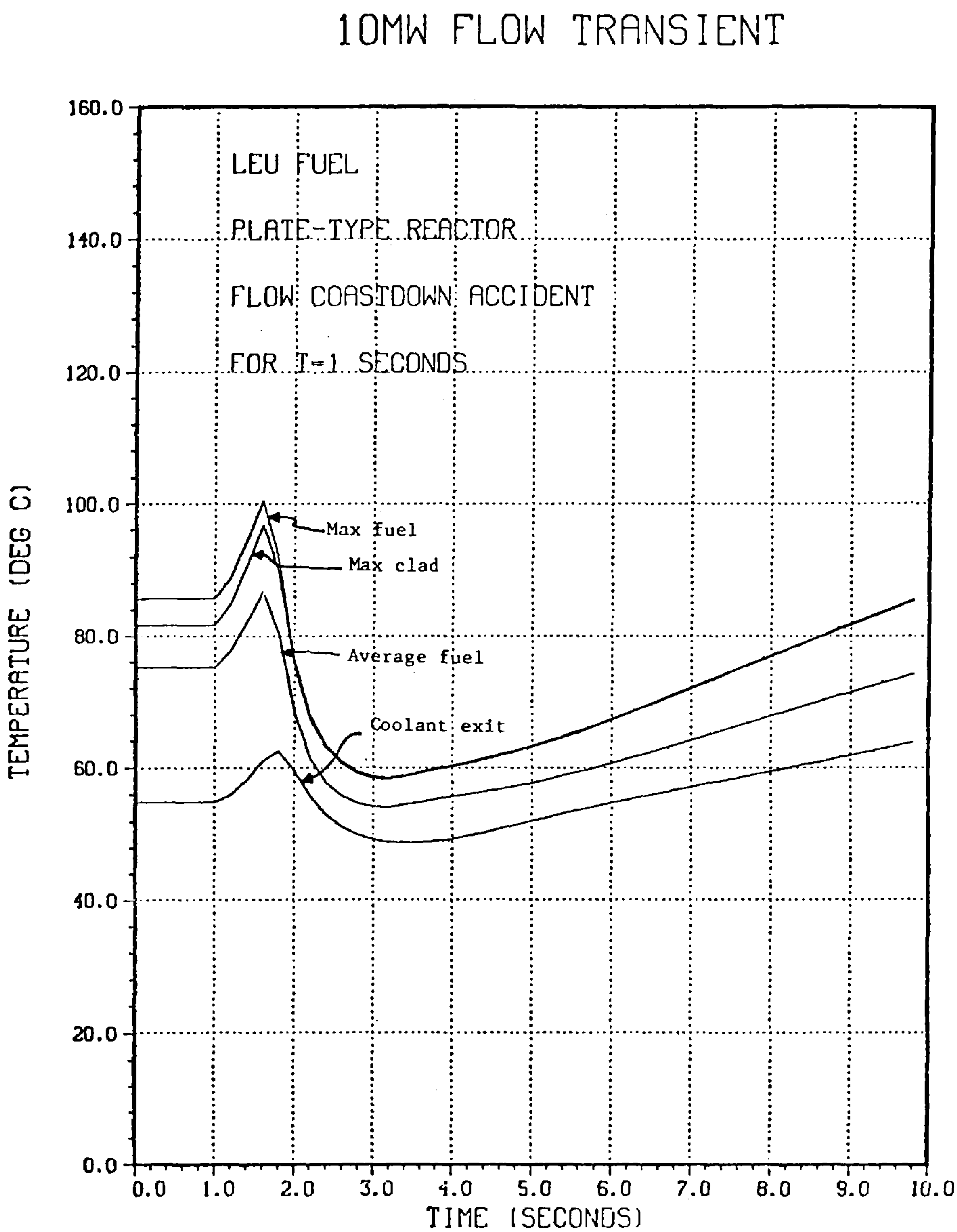

Figure 6. Loss of Flow Transient, LEU Fuel, T = 1 sec
Time Histroies of Fuel and Clad Temperatures

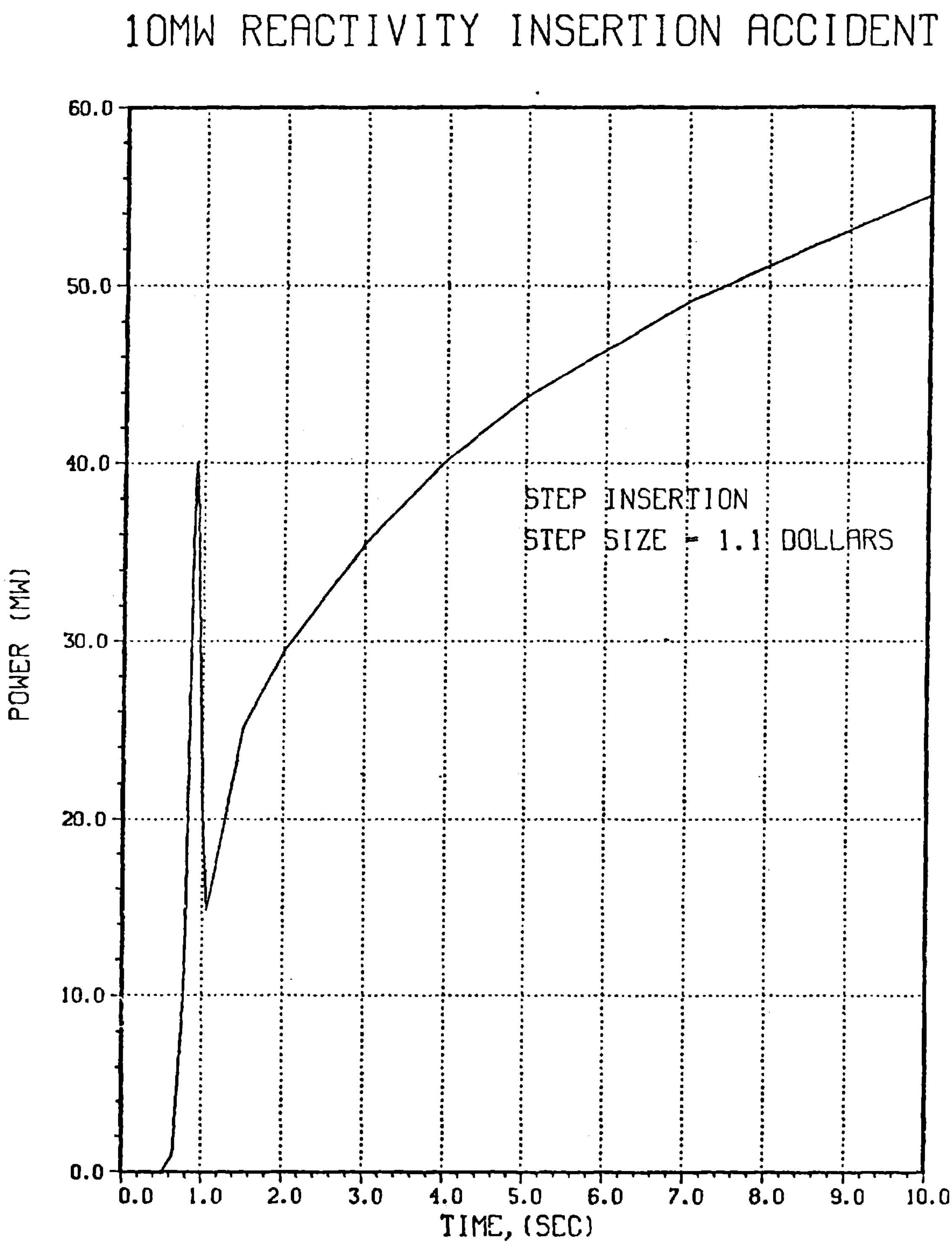

Figure 7. Step Reactivity Insertion, HEU Fuel, Step = \$1.10
Power vs. Time

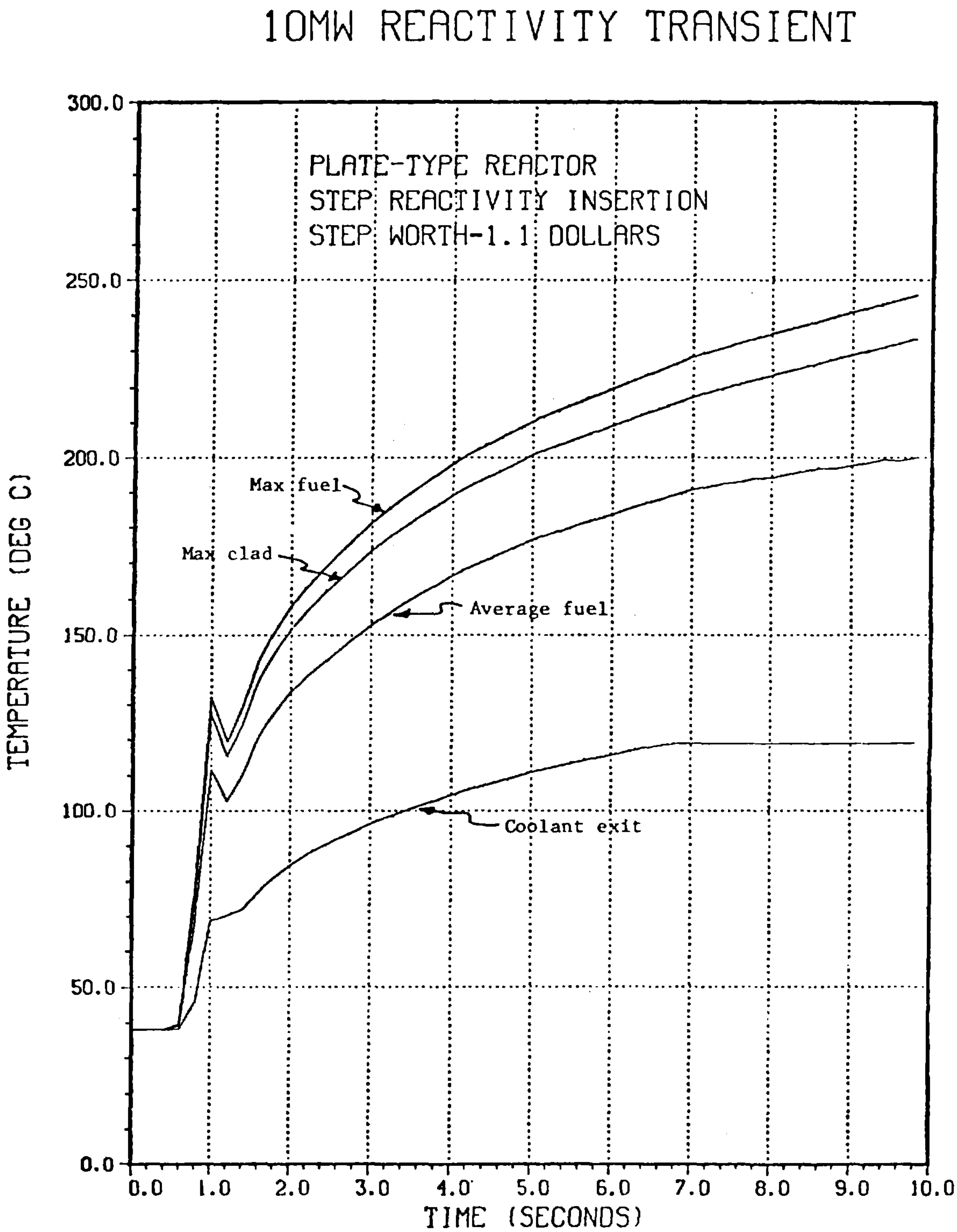

Figure 8. Step Reactivity Insertion, HEU Fuel, Step = $1.10
Fuel, Clad, and Coolant Exit Temperatures

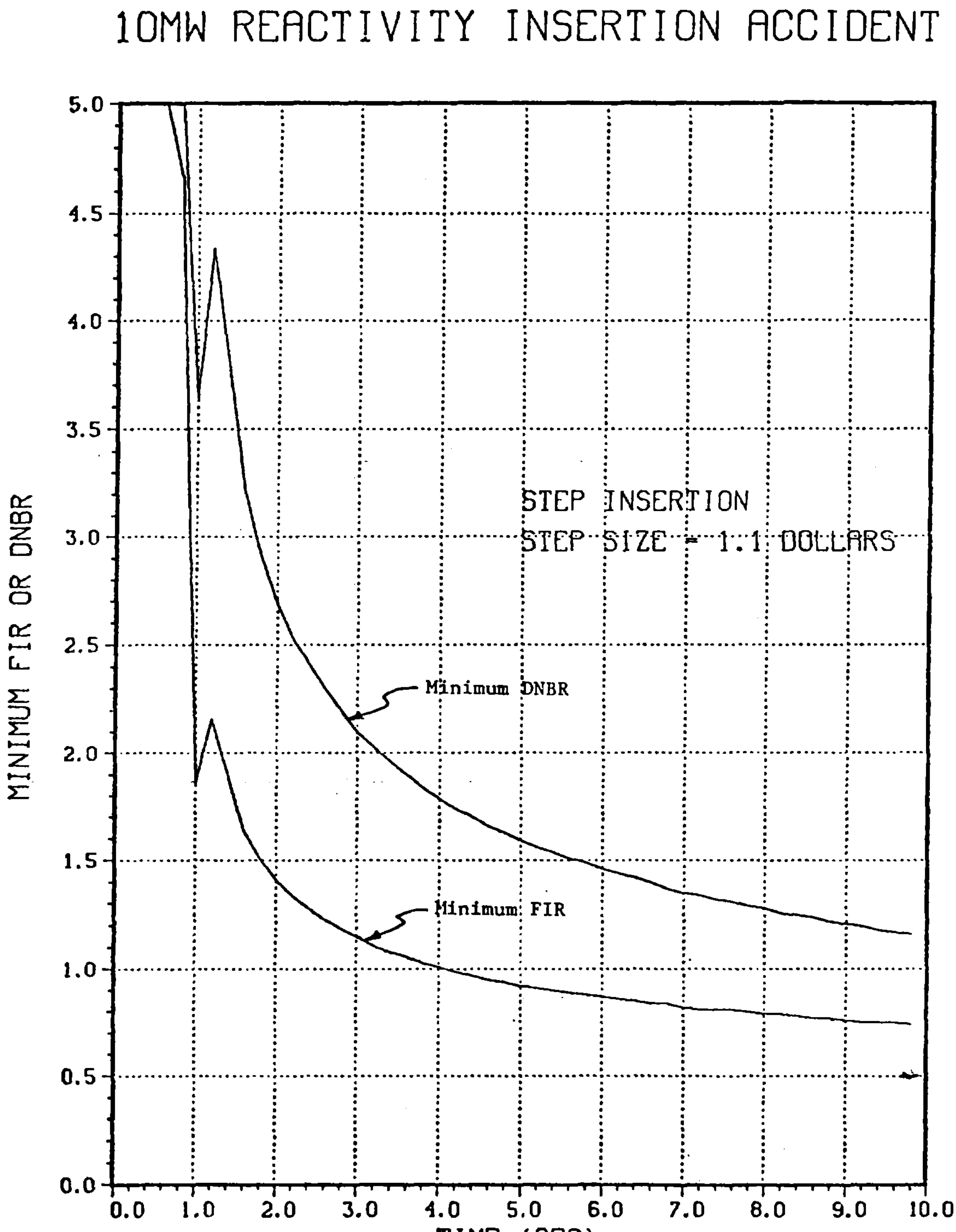

Figure 9. Step Reactivity Insertion, HEU Fuel, Step = $1.10
Minimum DNB and Flow Instability Ratios

10MW REACTIVITY INSERTION ACCIDENT

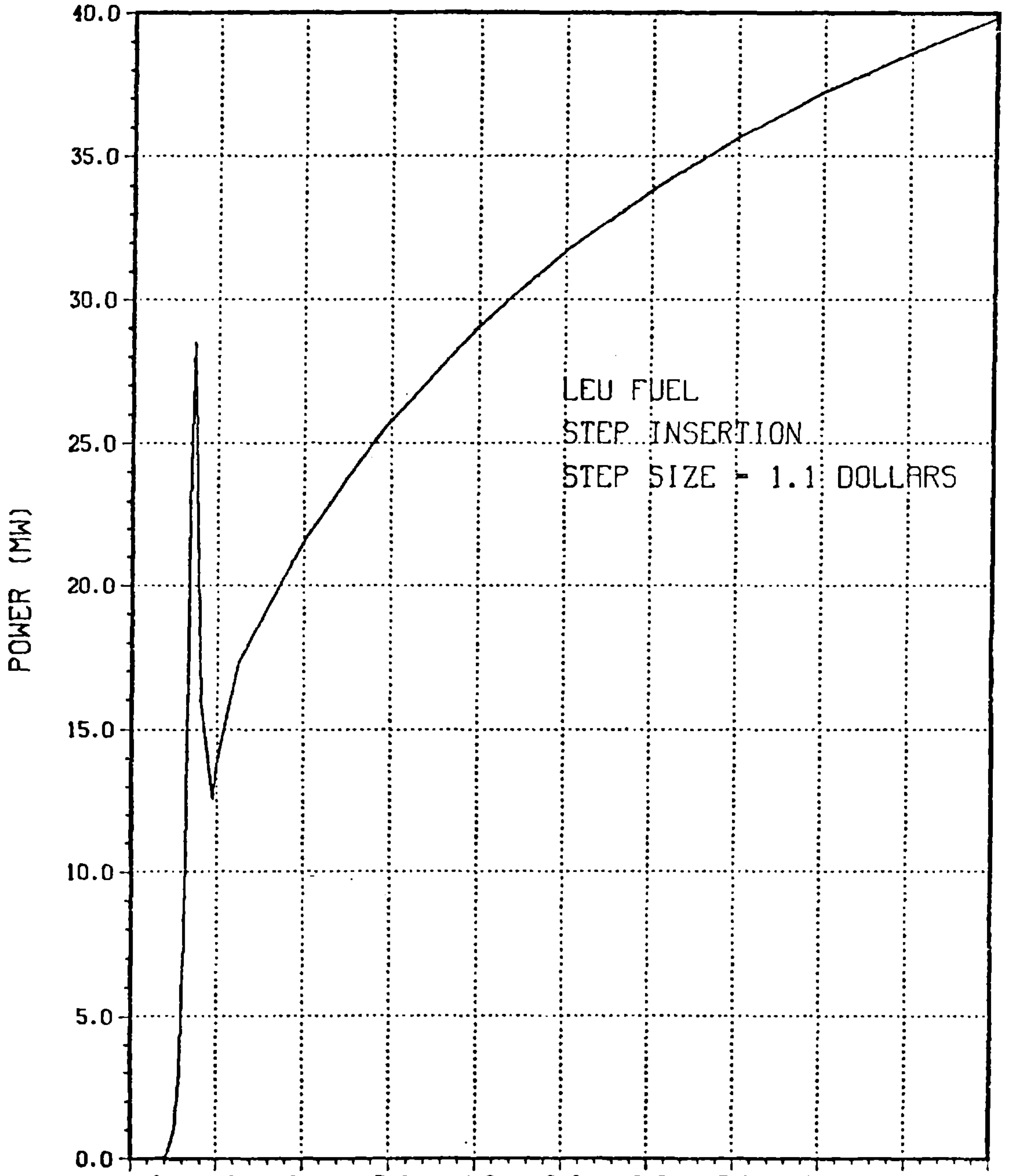

Figure 10. Step Reactivity Insertion, LEU Fuel, Step = $1.10
Power vs. Time

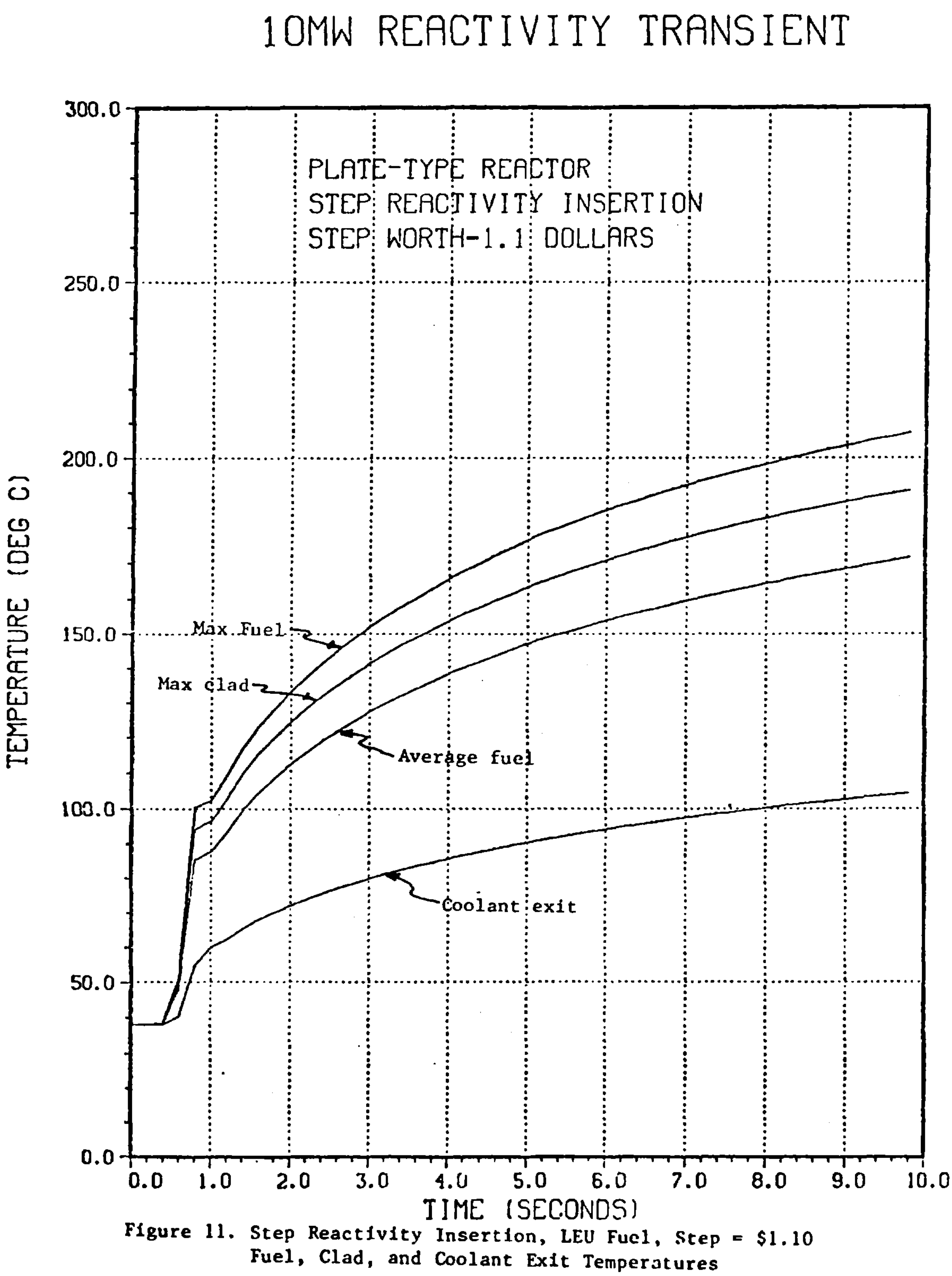

Figure 11. Step Reactivity Insertion, LEU Fuel, Step = $1.10
Fuel, Clad, and Coolant Exit Temperatures

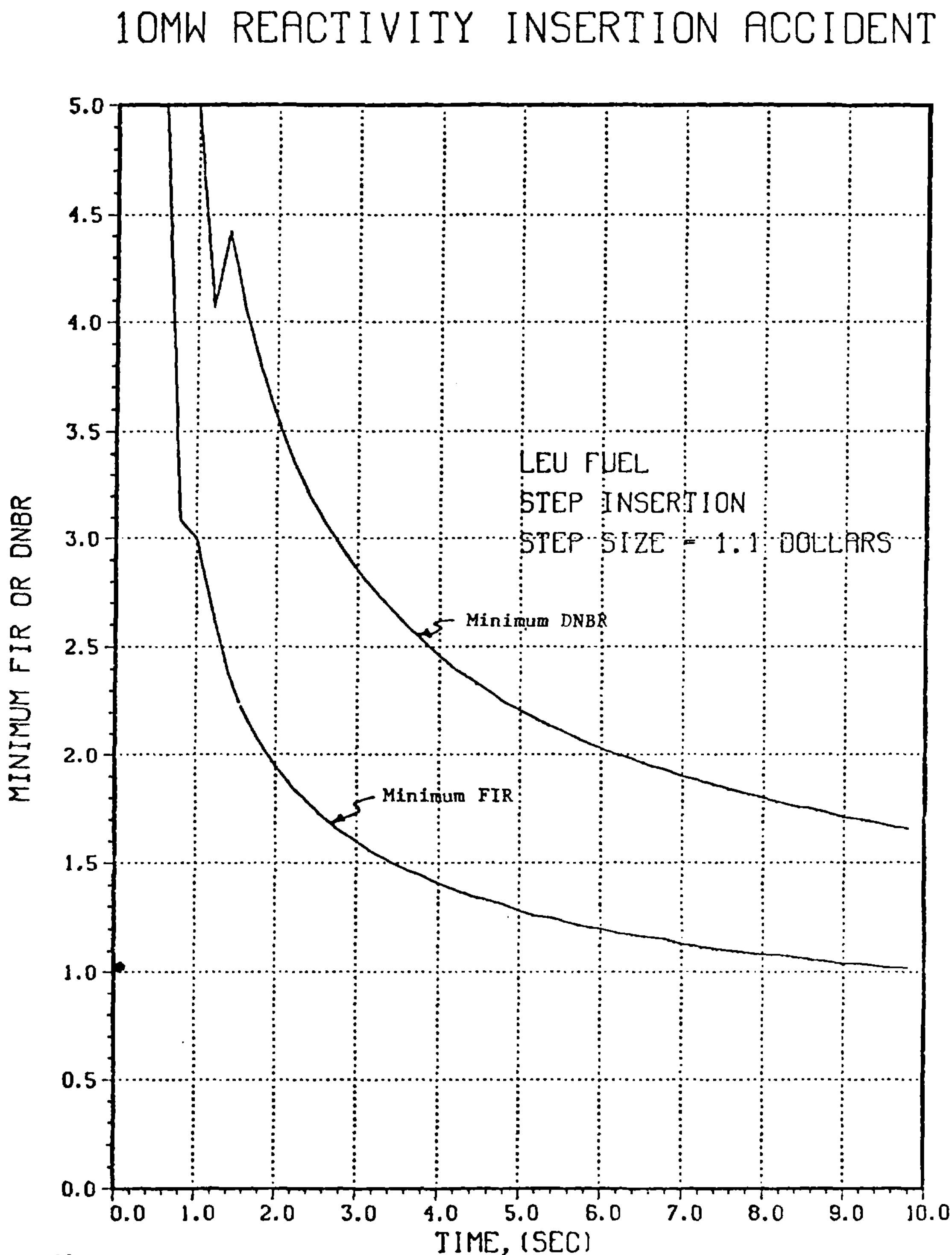

Figure 12. Step Reactivity Insertion, LEU Fuel, Step = $1.10
Minimum DNB and Flow Instability Ratios

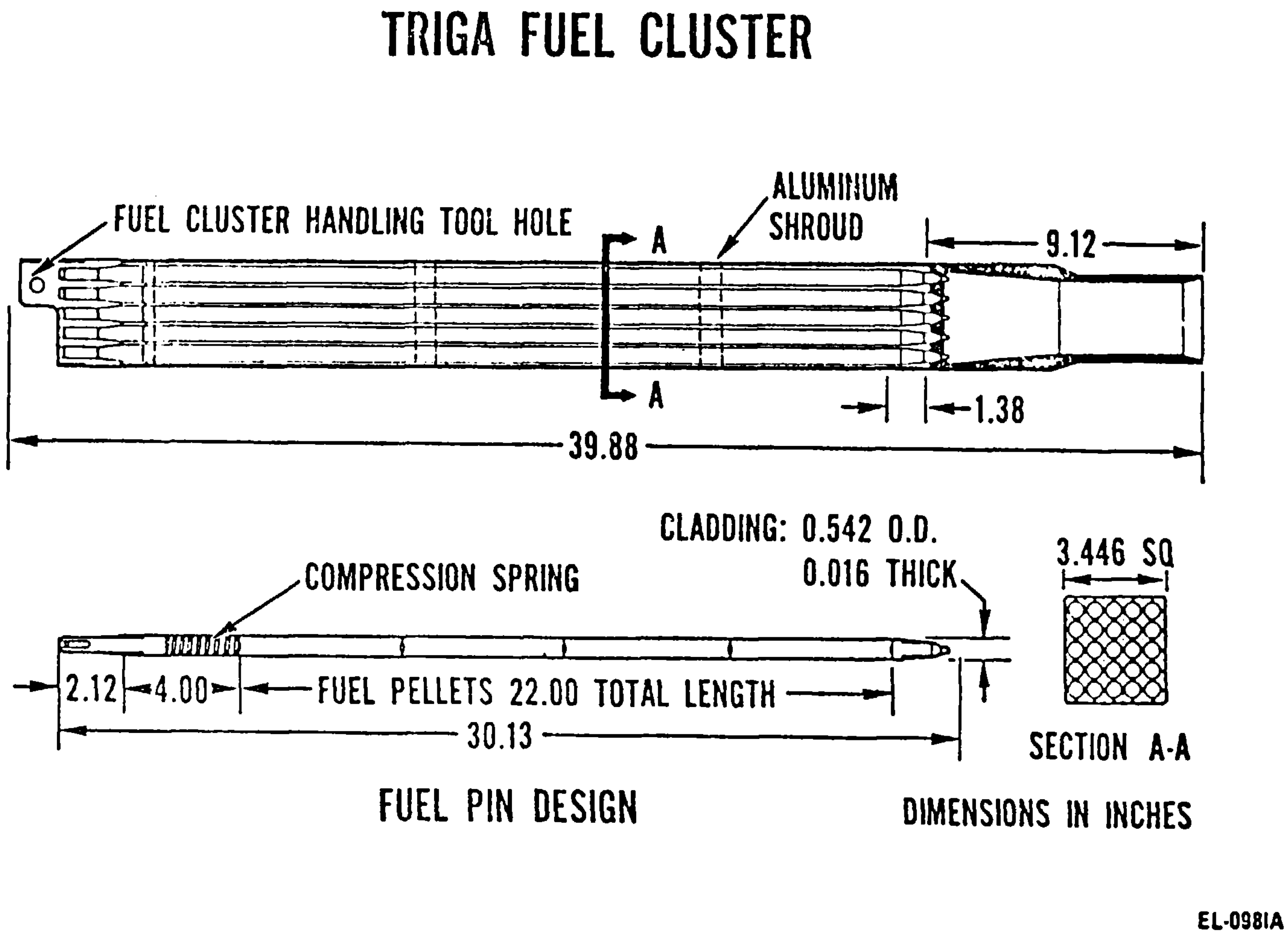

Figure 13. TRIGA 5 x 5 Fuel Cluster Design

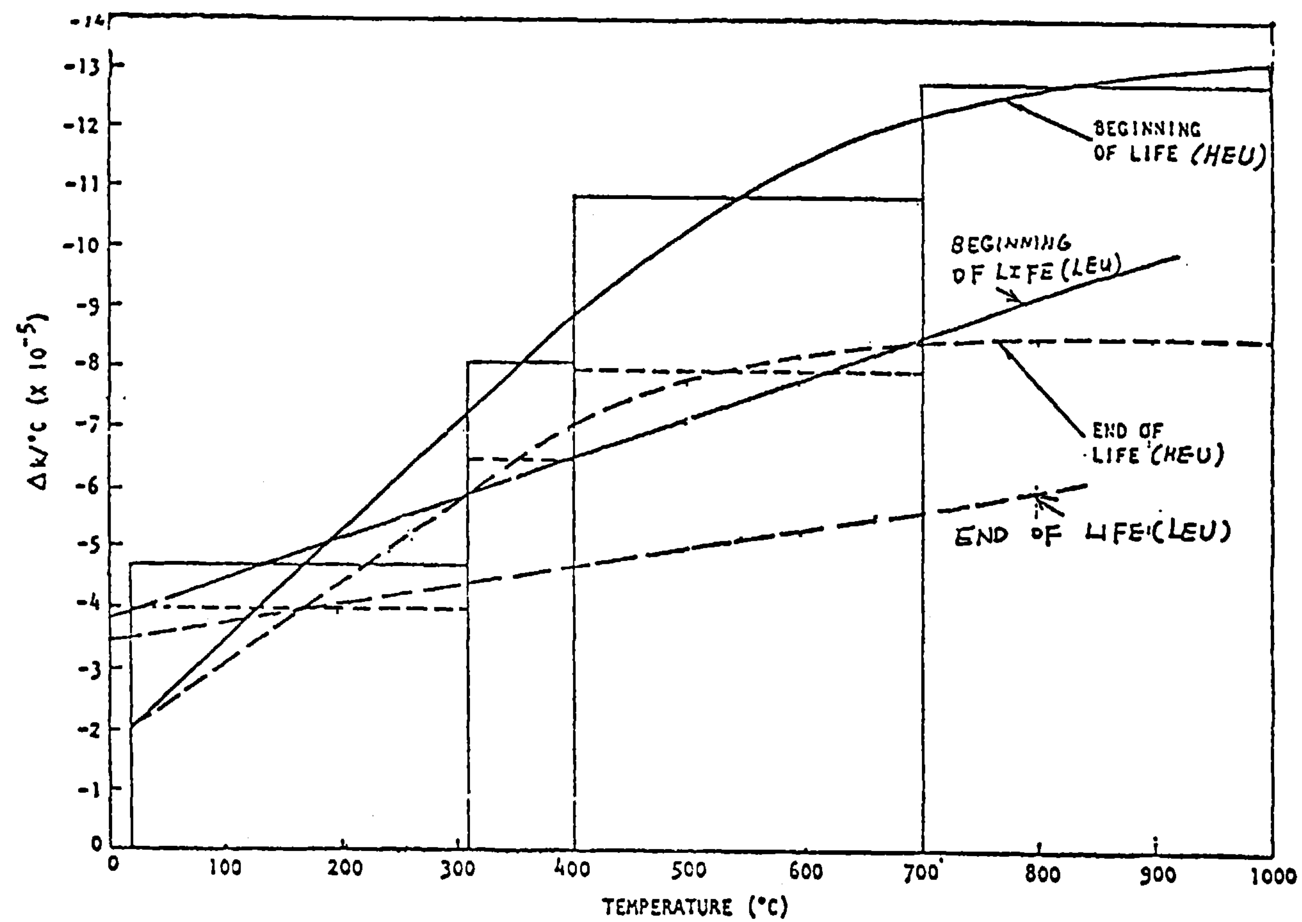

Figure 14. Temperature coefficient as a function of temperature for beginning-and end-of-life

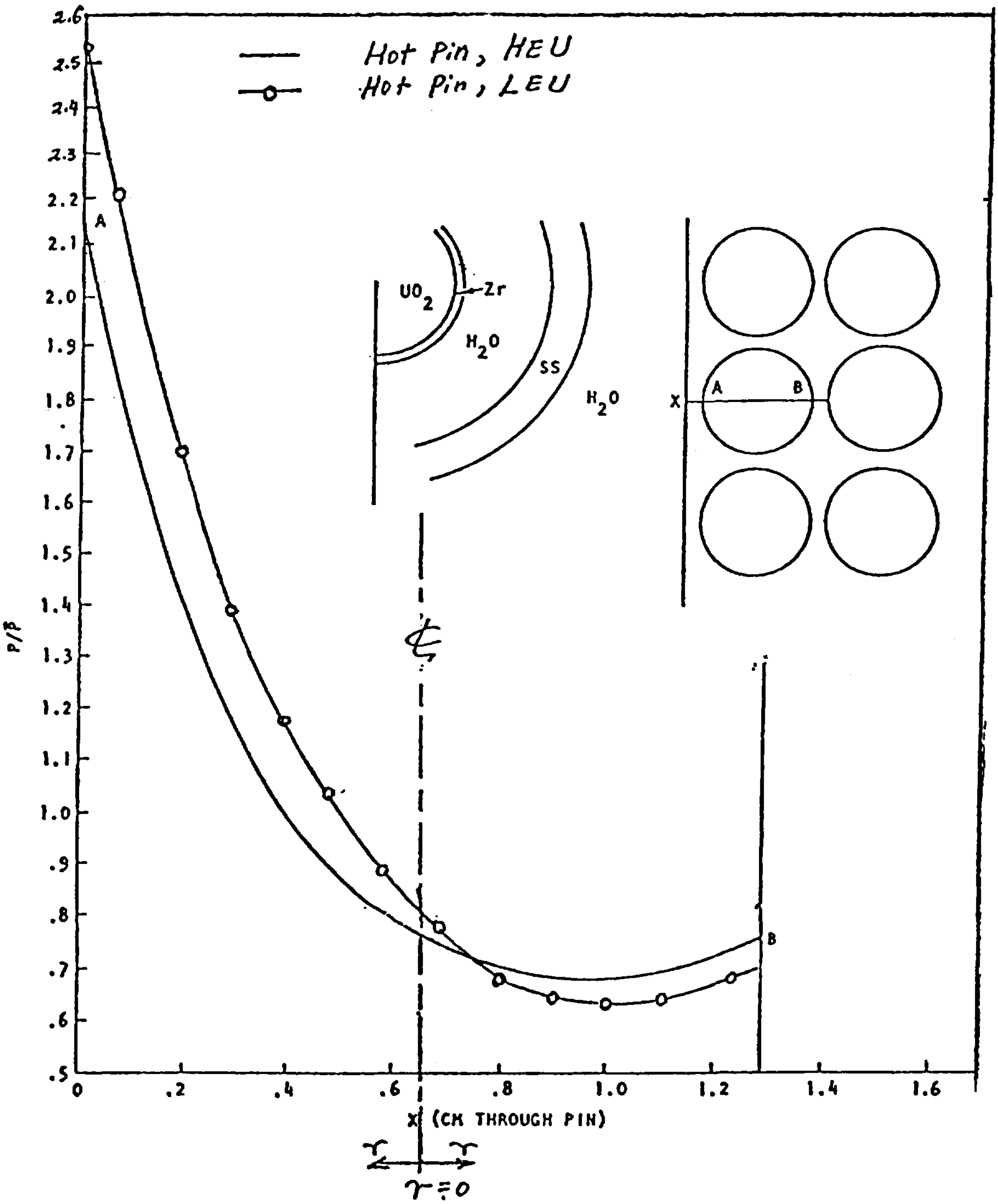

Figure 15. Relative Radial Power Profile Through Fuel Pin for Pin Adjacent to an In-core Experiment

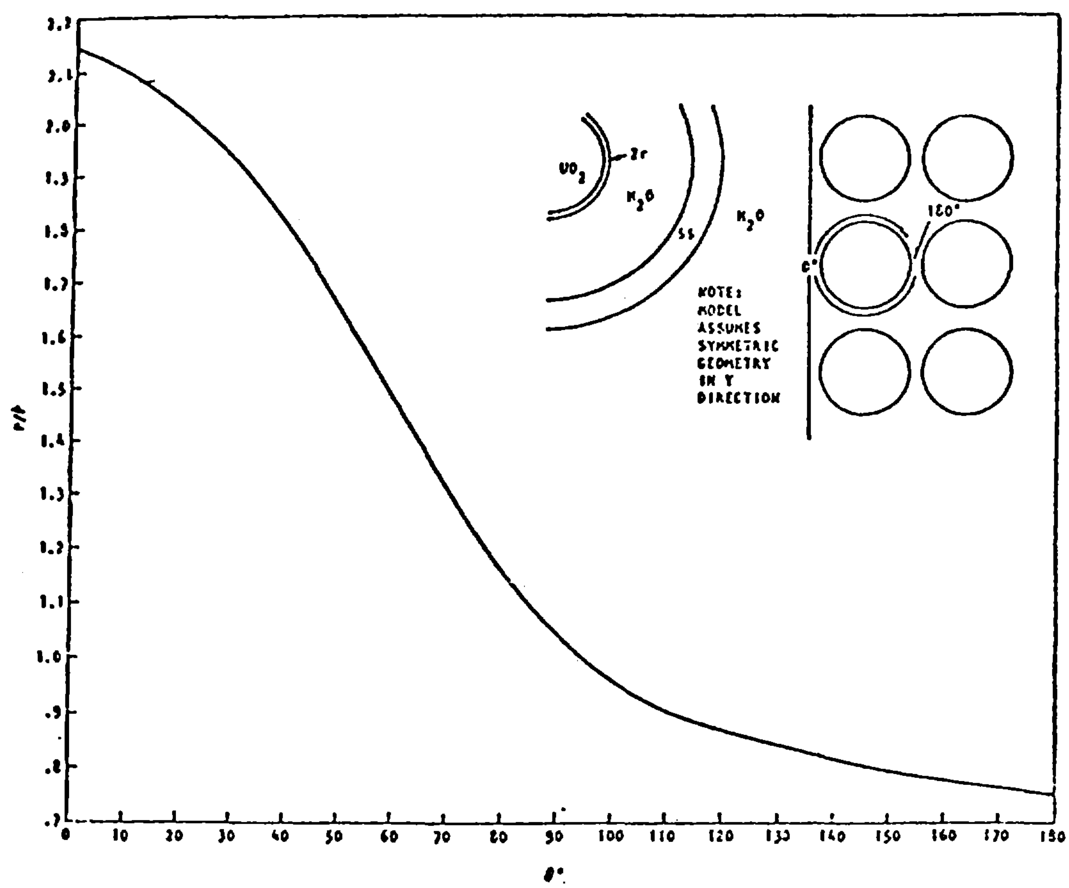

'Figure 16. Relative Azimuthal Power Profile on Fuel Pin Perimeter for Pin Adjacent to an In-core Experiment (taken from Ref. 7)

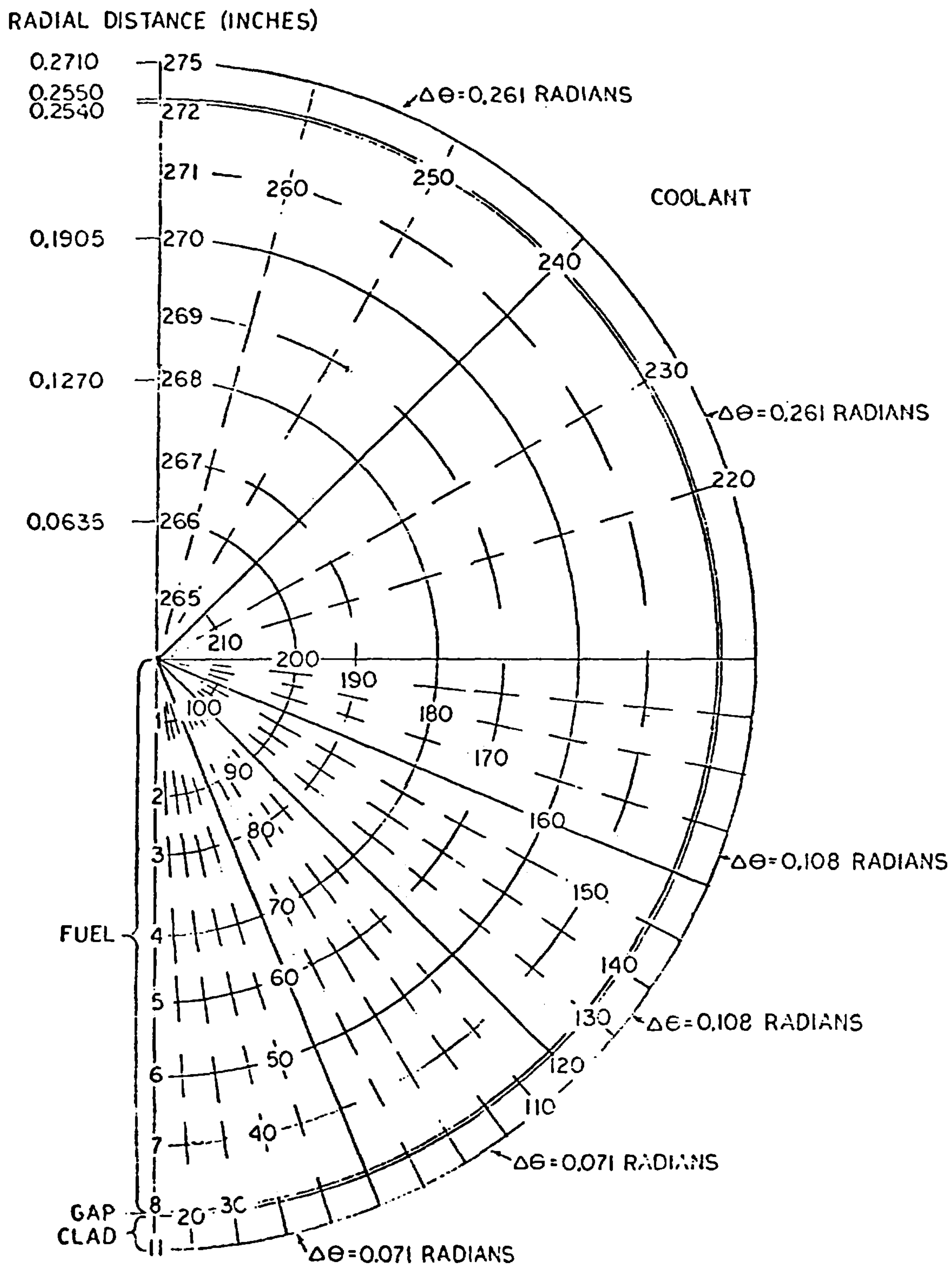

Figure 17. Spatial Nodes in HEATING5 Model of Hot Fuel Pin with Skewed Power Distribution

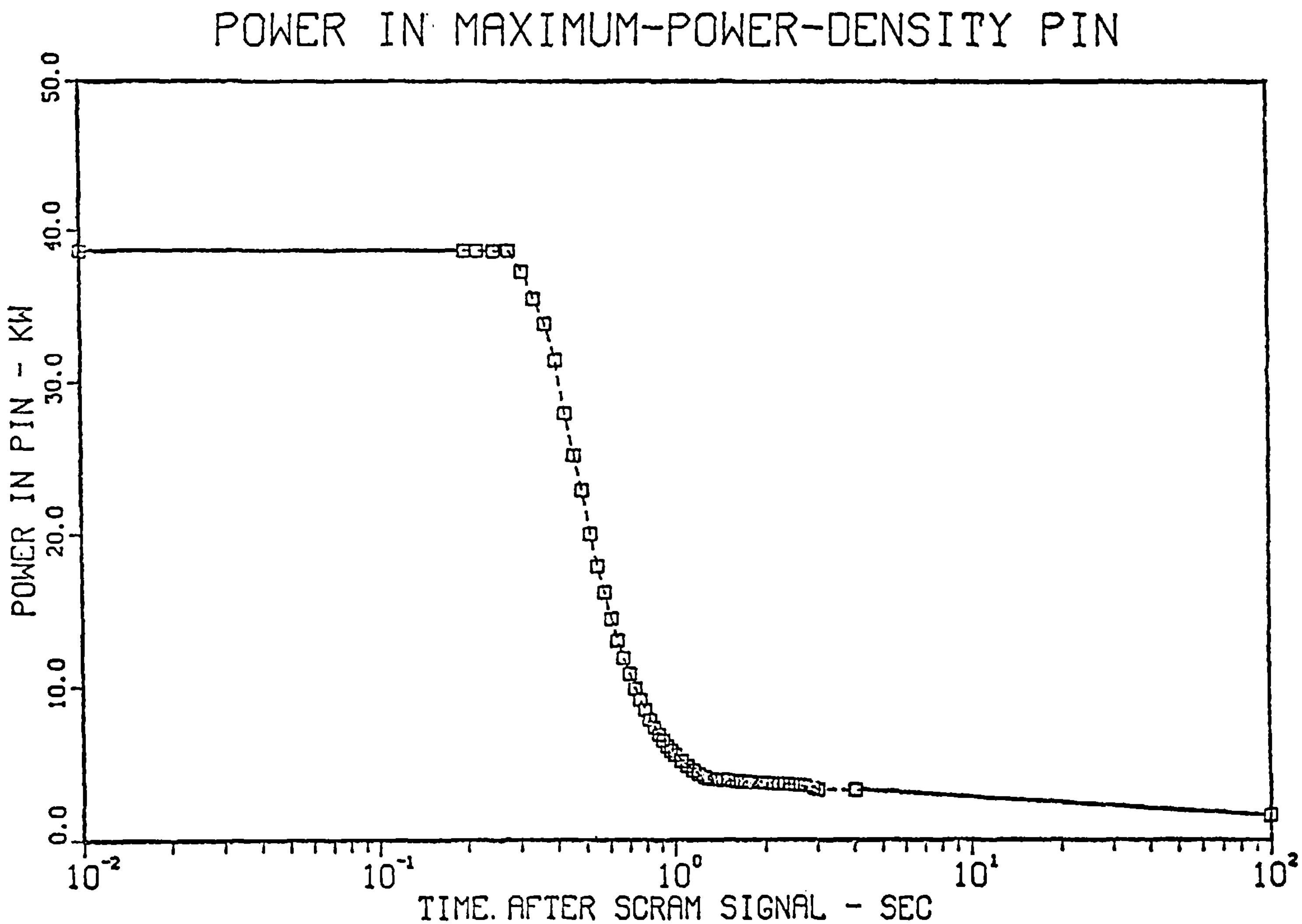

Figure 18. Power in Maximum-Power-Density Pin Following Scram
(Compare with Figure 5.3-1 of Ref. 7)

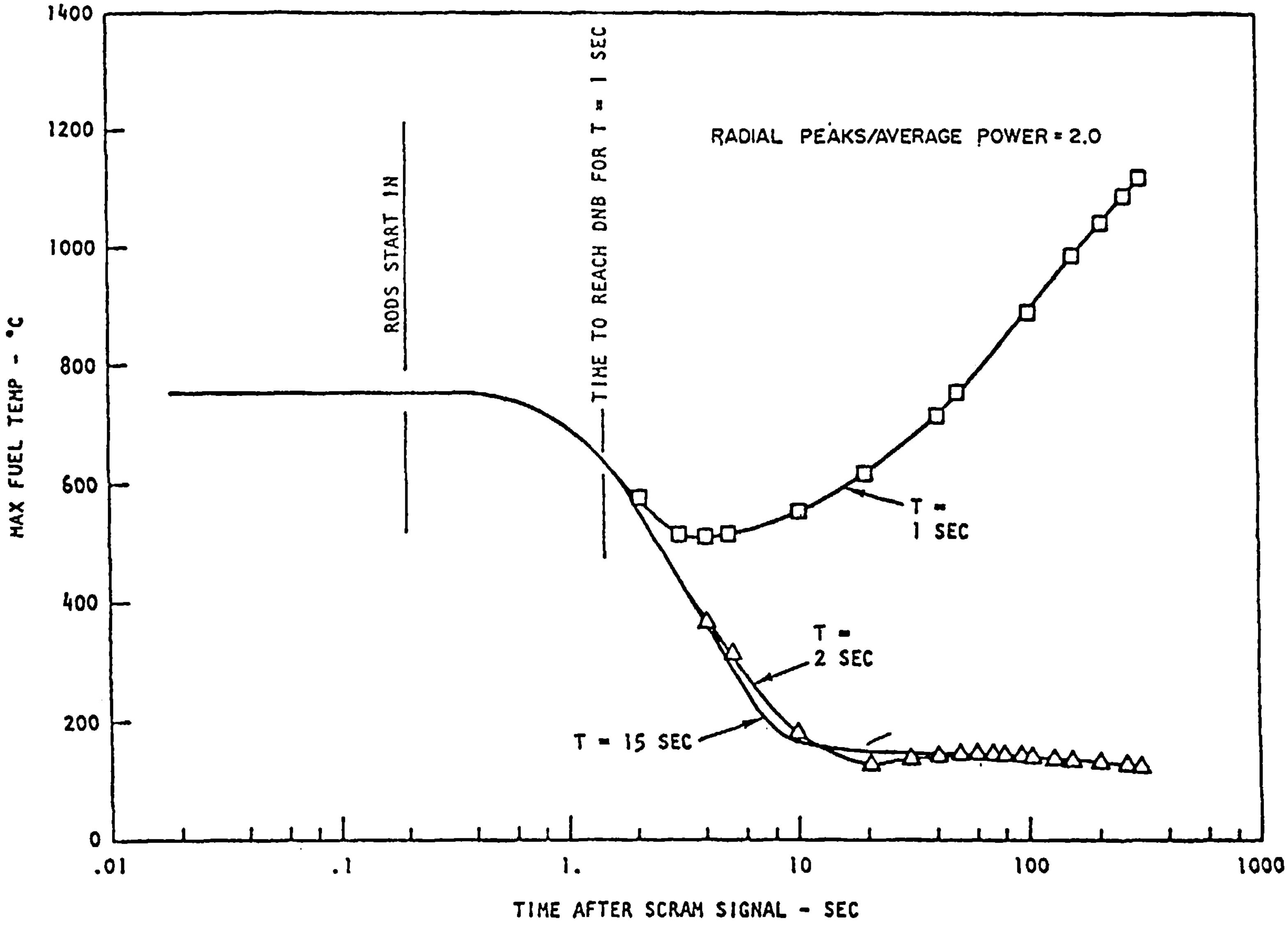

Figure 19. Maximum Fuel Temperatures During Flow Coastdown (from Ref. 7)

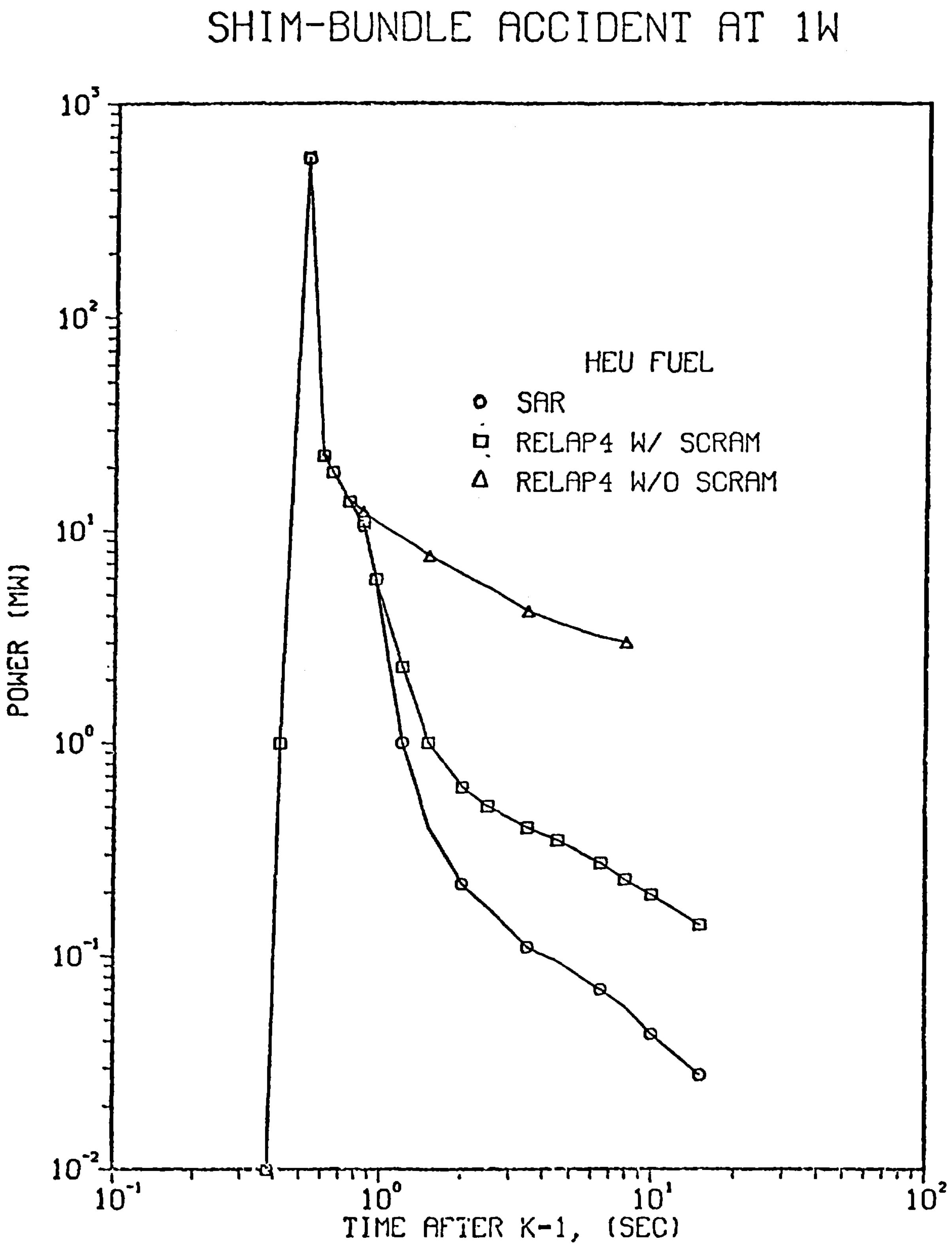

Figure 20. Time Histories of Power for the Shim-Bundle Accident at Low Power (HEU)

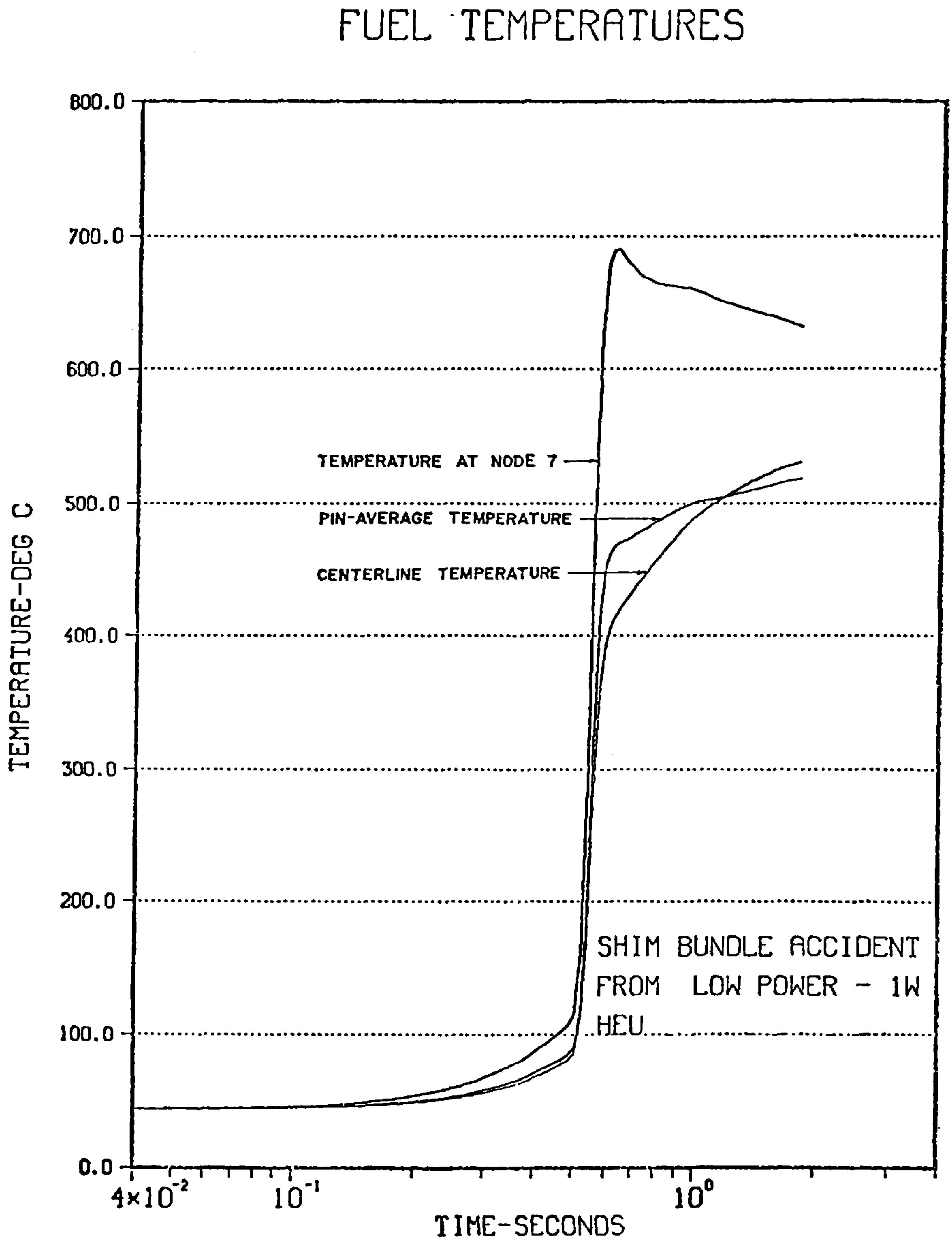

Figure 21. Time Histories of Fuel Temperatures in the Hottest Pin for the Shim-Bundle Accident at Low Power (HEU, core radial peaking factor = 1.9)

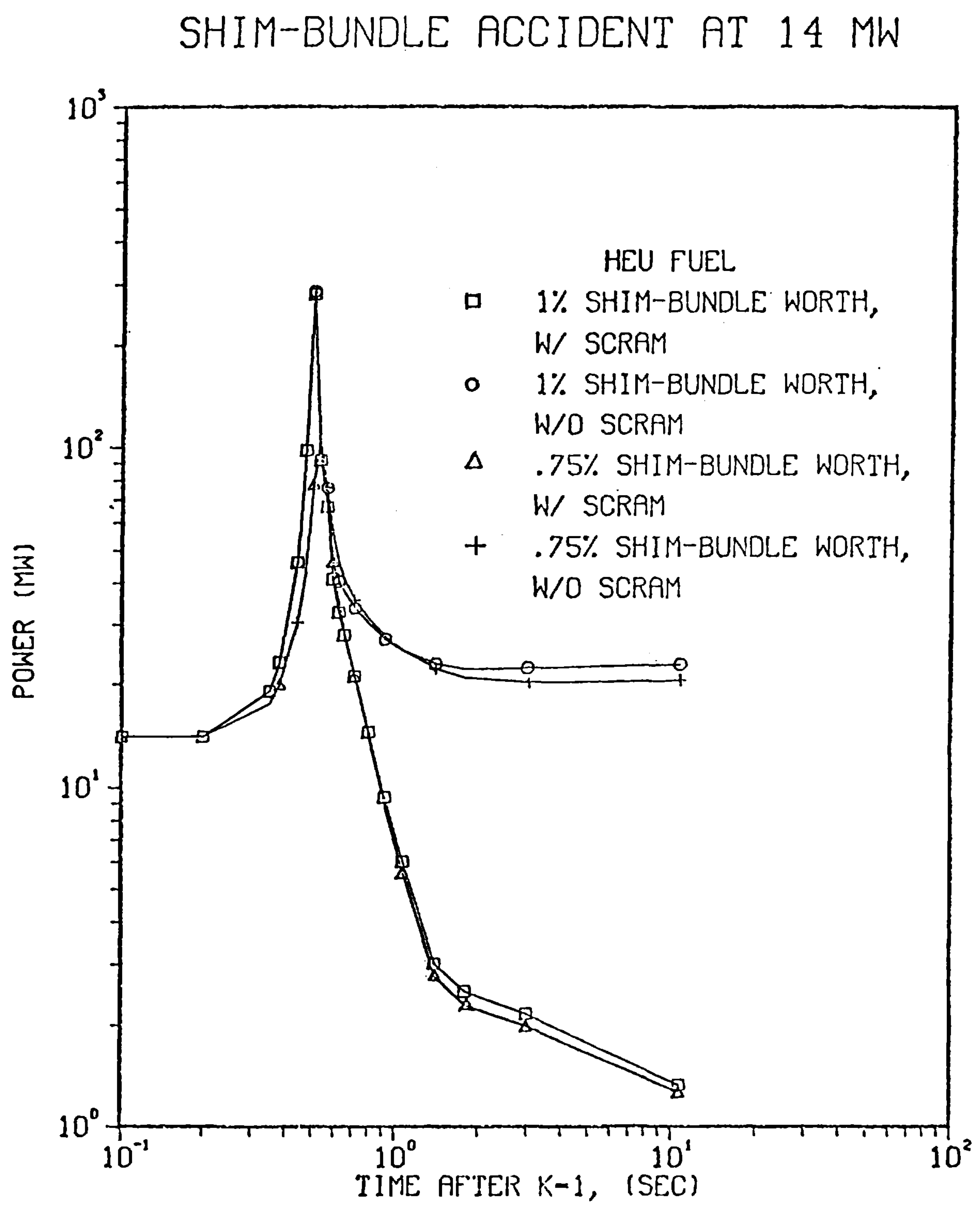

Figure 22. Time Histories of Power for the Shim-Bundle Accident at Full Power (HEU)

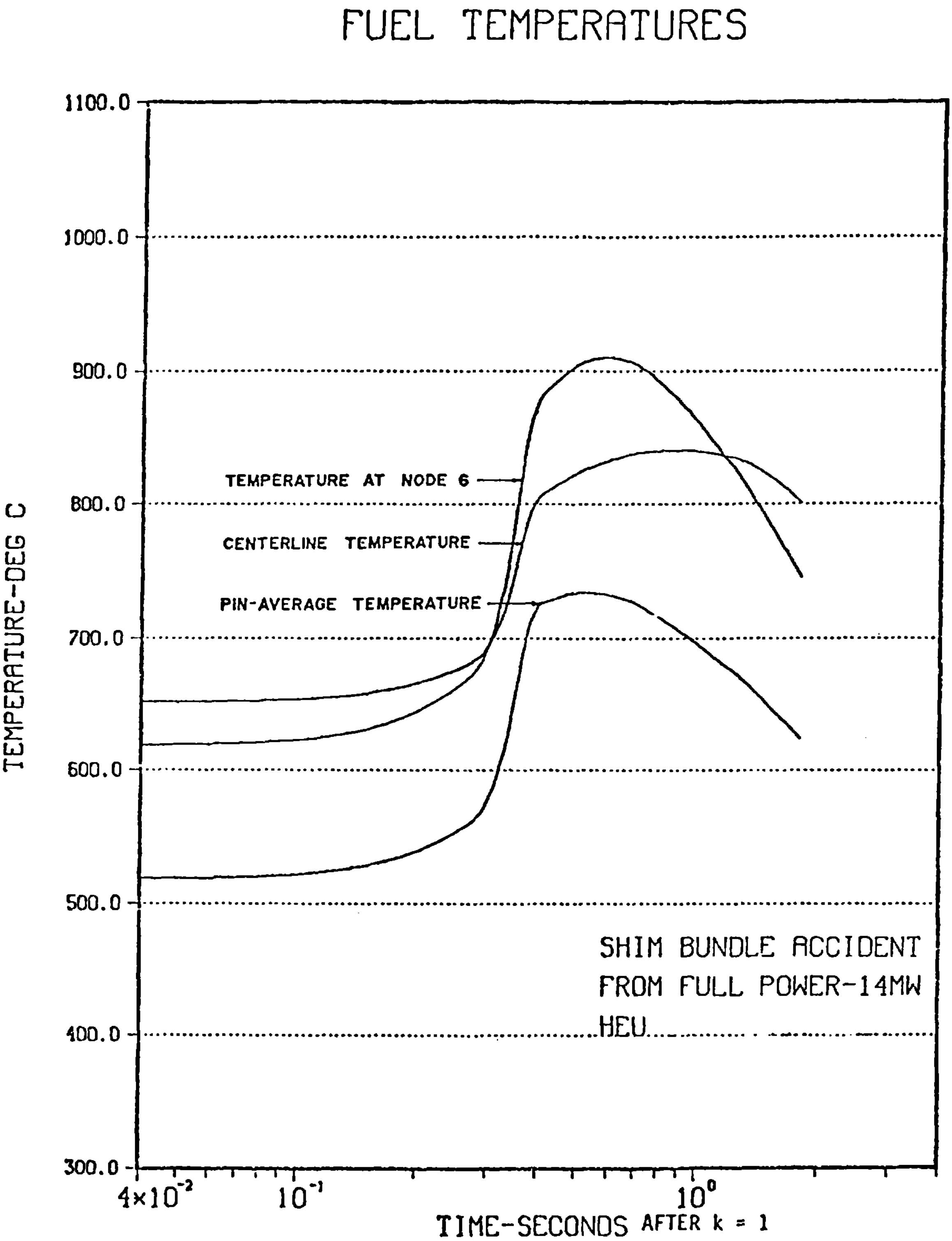

Figure 23. Time History of Fuel Temperatures in the Hottest Pin for the Shim-Bundle Accident at Full Power (HEU, 1% δk/k, core radial peaking factor = 1.9)

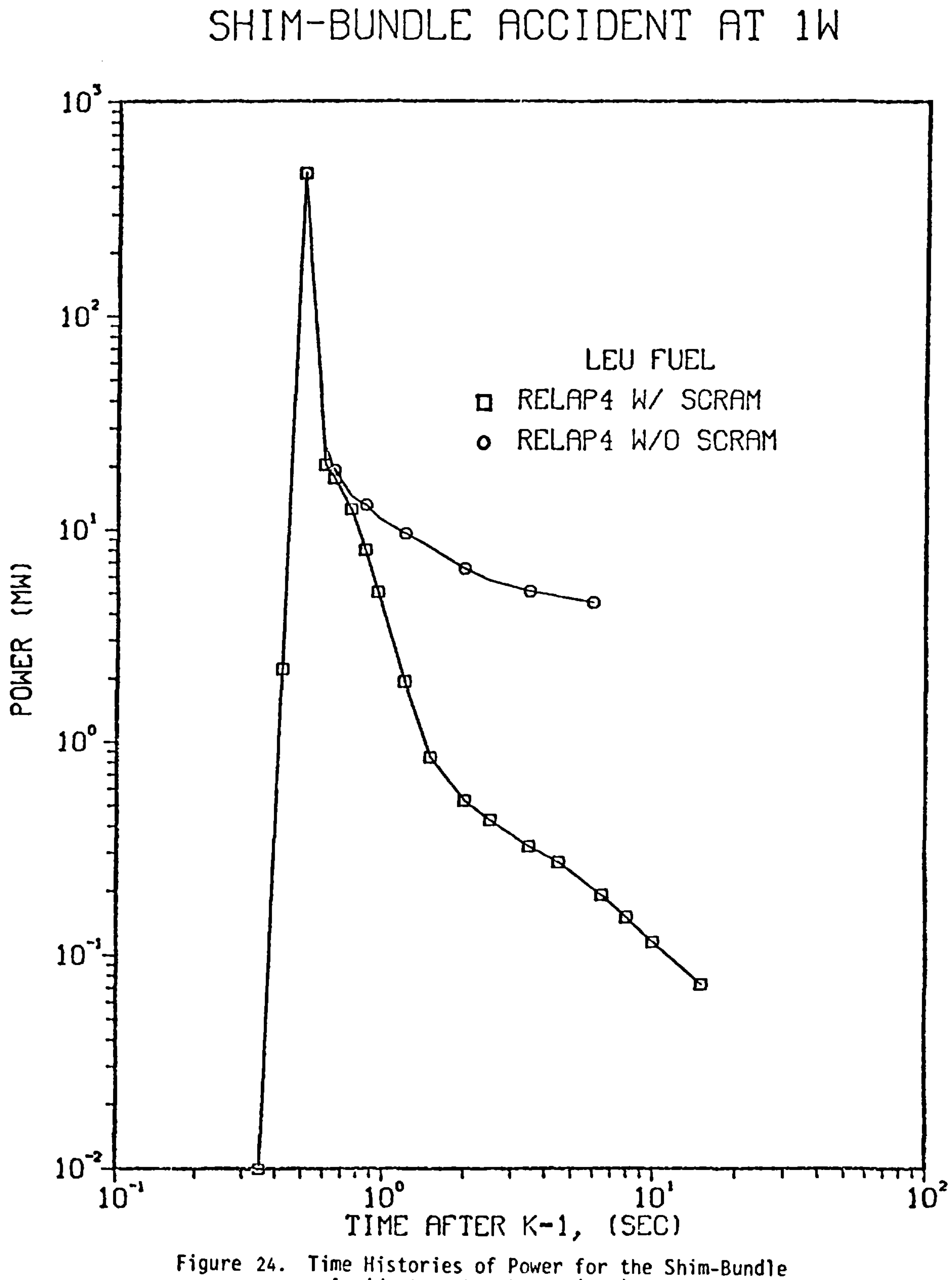

Figure 24. Time Histories of Power for the Shim-Bundle Accident at Low Power (LEU)

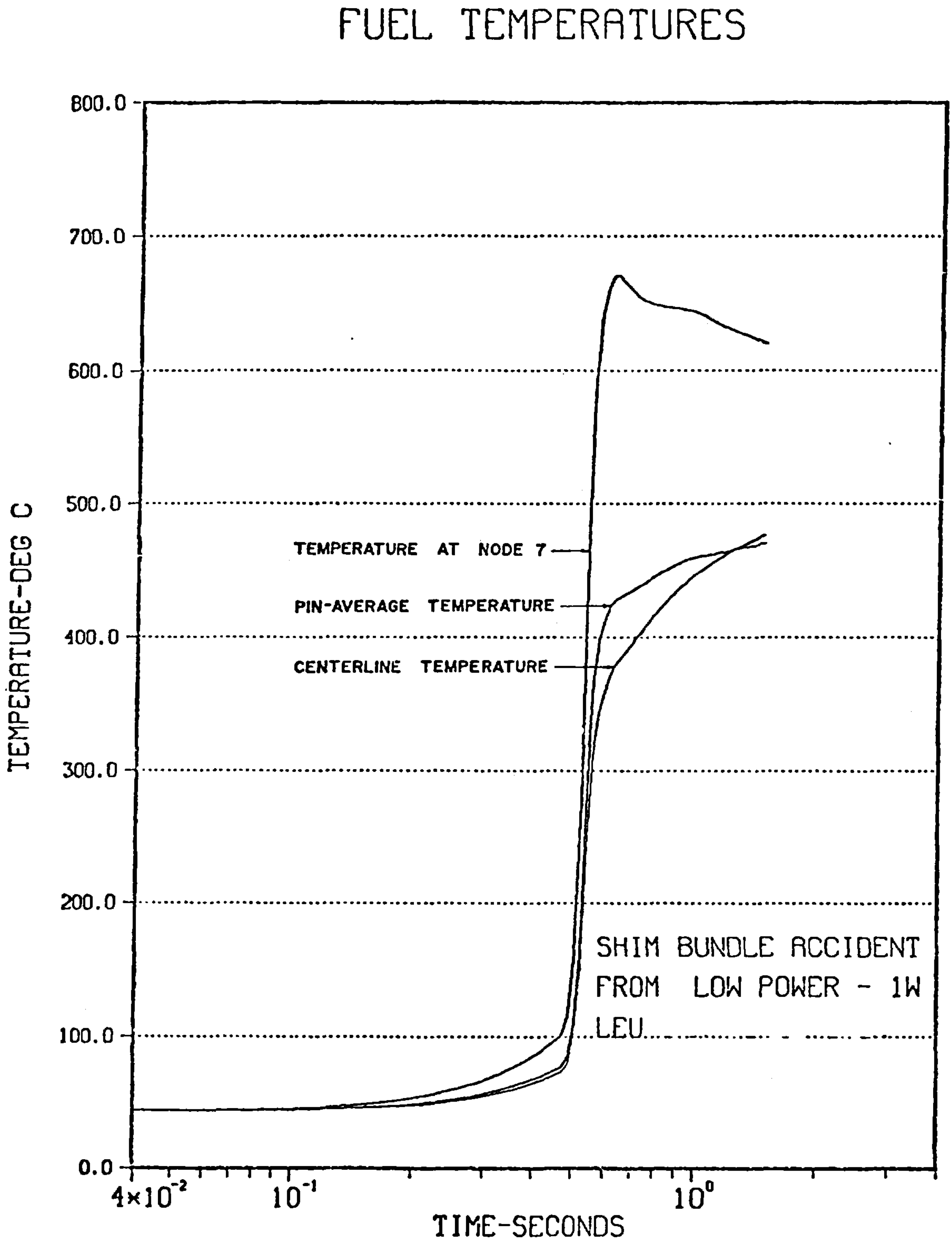

Figure 25. Time Histories of Fuel Temperatures in the Hottest Pin for the Shim-Bundle Accident at Low Power (LEU, core radial peaking factor = 1.9)

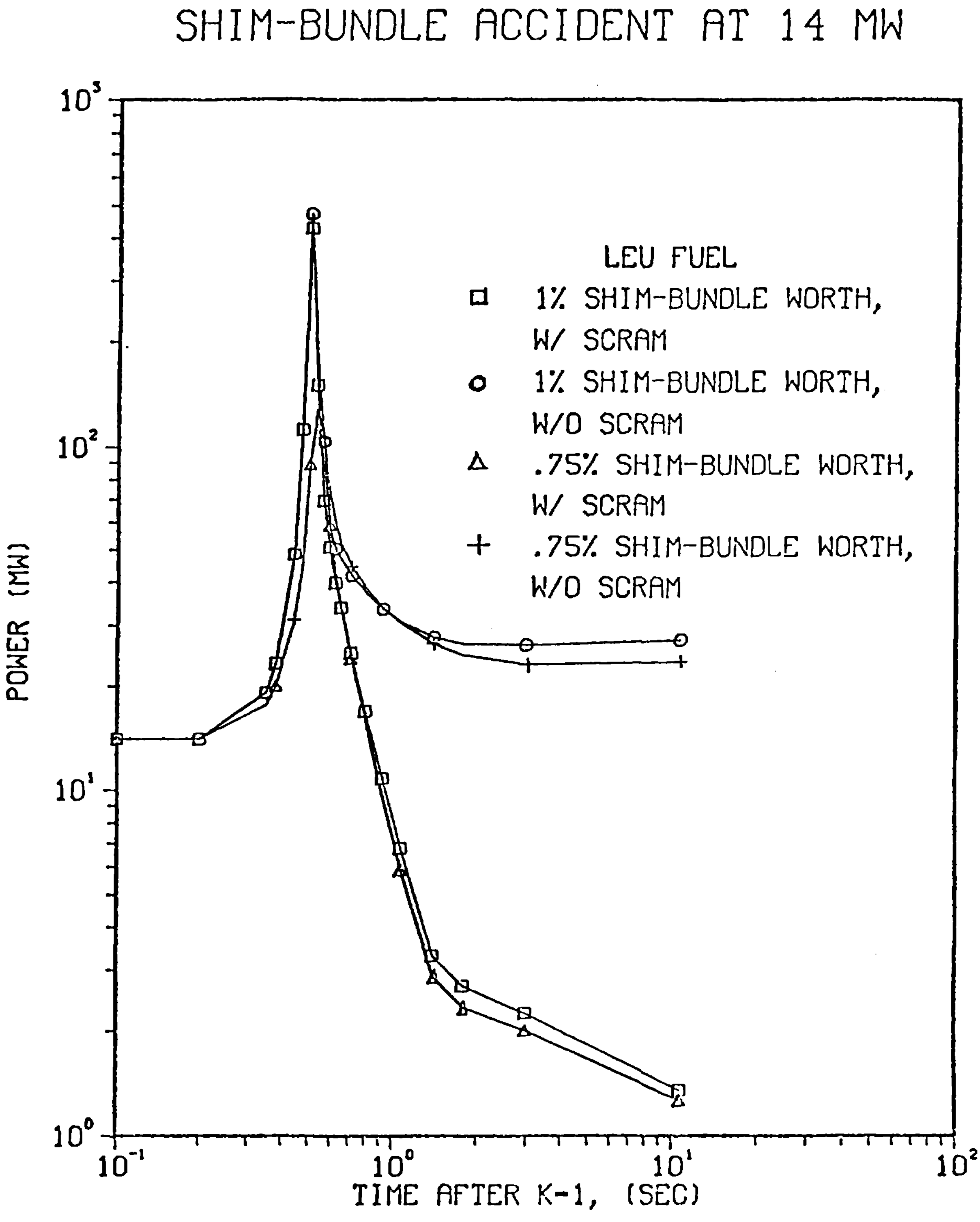

Figure 26. Time Histories of Power for the Shim-Bundle Accident at Full Power (LEU)

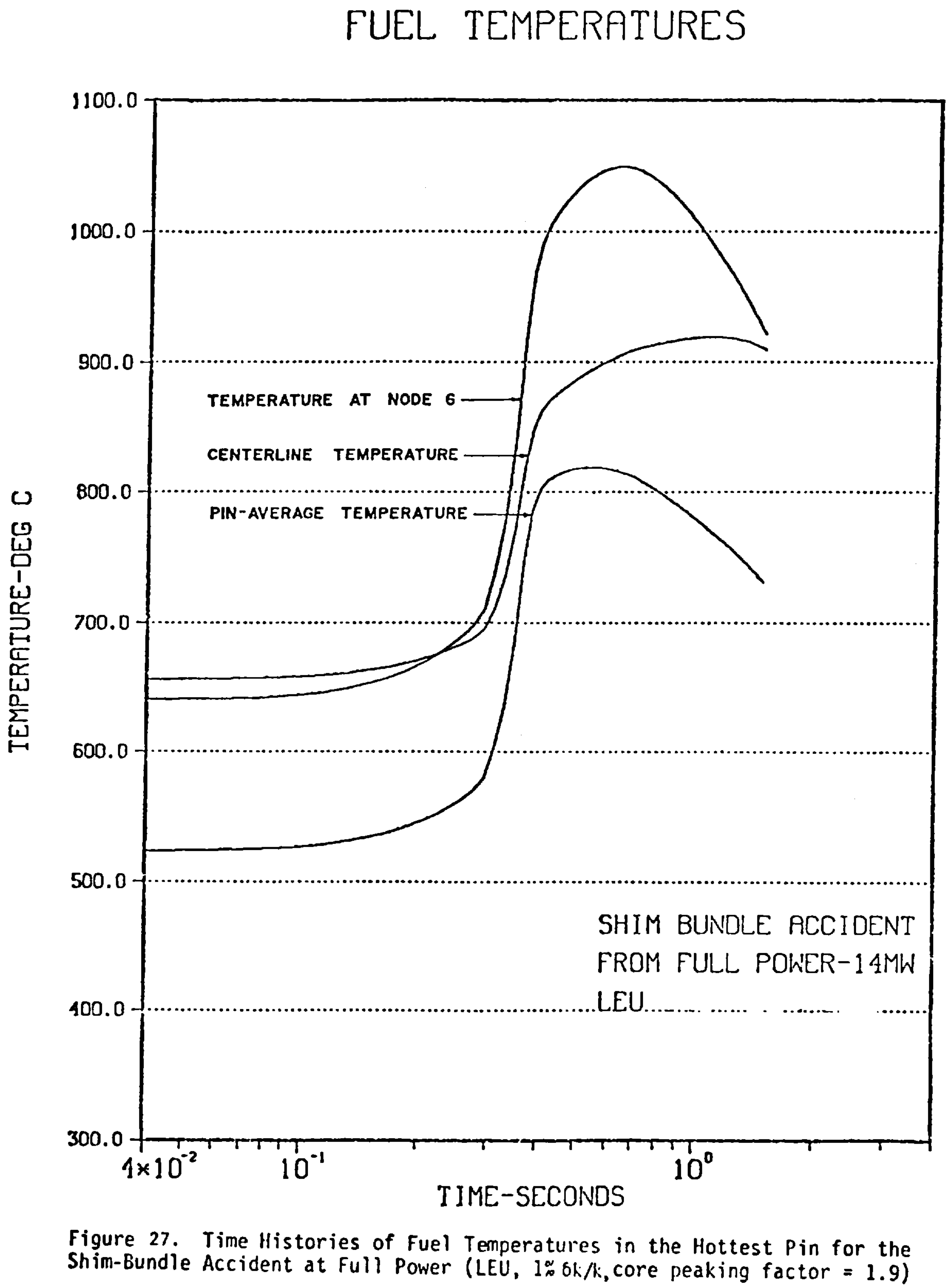

Figure 27. Time Histories of Fuel Temperatures in the Hottest Pin for the Shim-Bundle Accident at Full Power (LEU, 1% δk/k, core peaking factor = 1.9)